excitation wavelength of 360 nm and an emission wavelength of 465 nm and the 50% inhibitory concentration (IC_{50}) was calculated.

Neutralization assay with human sera. Human sera were collected in 1999 or 2009 from donor group 1 (age range: 50–112 years as of 2009, mean = 92.7 ± 15.0 years) or 2 (age range: 20–68 years as of 2009, mean = 48.2 ± 23.7 years), respectively. These sera were treated with receptor-destroying enzyme (DENKA SEIKEN CO.) to remove inhibitors of influenza virus replication. One hundred $TCID_{50}$ (50% tissue culture infectious dose) of CA04 and KUTK-4 were pre-incubated with twofold serial dilutions of treated sera, incubated for 60 min on MDCK cells, which were then observed for cytopathic effects to determine the neutralizing activity of the test sera. Our research protocol was approved by the Research Ethics Review Committee of the Institute of Medical Science, the University of Tokyo (approval numbers: 21-6-0428 for donor group 1; 21-7-0529 for donor group 2).

Immunofluorescence microscopy. MDCK cells were infected with CA04, KUTK-4, or WSN and fixed with 4% paraformaldehyde 16–24 h later. Infected cells were incubated with the following primary antibodies: mouse anti-HA (7B1b), anti-HA (IVC102), or mouse anti-HA (WS3-54) antibody against CA04, KUTK-4 or WSN, respectively. Cells were then incubated with Alexa Fluor 488 goat anti-mouse immunoglobulin G (Invitrogen), and examined with a confocal laser-scanning microscope (LSM510META; Carl Zeiss).

Electron microscopy. MDCK cells were infected with CA04, KUTK-4 or WSN at a multiplicity of infection of 10. At 16–24 h after infection, cells were processed for ultrathin section electron microscopy and scanning electron microscopy as described previously[19,21].

19. Noda, T. *et al.* Architecture of ribonucleoprotein complexes in influenza A virus particles. *Nature* **439**, 490–492 (2006).
20. Kiso, M. *et al.* Resistant influenza A viruses in children treated with oseltamivir: descriptive study. *Lancet* **364**, 759–765 (2004).
21. Neumann, G. *et al.* Ebola virus VP40 late domains are not essential for viral replication in cell culture. *J. Virol.* **79**, 10300–10307 (2005).

Analytical Biochemistry 389 (2009) 80–82

Contents lists available at ScienceDirect

Analytical Biochemistry

journal homepage: www.elsevier.com/locate/yabio

Notes & Tips

Application of retrovirus-mediated expression cloning for receptor screening of a parasite

Kyousuke Kobayashi [a], Kentaro Kato [a,*], Tatsuki Sugi [a], Daisuke Yamane [a], Masayuki Shimojima [b], Yukinobu Tohya [a], Hiroomi Akashi [a]

[a] Department of Veterinary Microbiology, Graduate School of Agricultural and Life Sciences, University of Tokyo, Bunkyo-ku, Tokyo 113-8657, Japan
[b] Division of Virology, Department of Microbiology and Immunology, Institute of Medical Science, University of Tokyo, Minato-ku, Tokyo 108-8639, Japan

ARTICLE INFO

Article history:
Received 7 February 2009
Available online 12 March 2009

ABSTRACT

Retrovirus-mediated expression cloning has been applied in both virology and cell biology. Although there is some difficulty in applying this technique to screening for a receptor recognized by an intracellular parasite, we modified the conventional method to identify a putative receptor for the *Plasmodium falciparum* BAEBL protein. We show that this method is effective in screening for a parasite receptor.

To develop effective means of preventing and treating infectious diseases, it is important to understand the interactions between a pathogen and its host. For a pathogen to invade host cells, such as viruses or protozoans, the pathogen must recognize a receptor on the surface of the host cells.

Various methods have been developed for identifying the partner that interacts with a particular molecule. One such method is retrovirus-mediated expression cloning [1–3], which has been applied to studies in both virology [4,5] and cell biology [6]. We sought to apply this method to screen for the receptor recognized by an intracellular apicomplexan parasite.

Shimojima and coworkers [4] identified CD134 as the primary receptor for feline immunodeficiency virus (FIV)[1] using the following procedure. First, a complementary DNA (cDNA) library made from the FIV-sensitive cell line MYA-1 was transduced to the FIV-insensitive cell line P3S63Ag8U.1 (P3U1) using a retrovirus vector. As a result, a proportion of the P3U1 cells expressed the receptor. To isolate the receptor-expressing cells, the transduced P3U1 cells were panned using a dish coated with FIV particles. The receptor molecule was determined from the sequence of feline CD134 cDNA amplified by polymerase chain reaction (PCR) using genomic DNA from an isolated cell clone as the template and vector-specific primers.

This procedure has two problems before it can be applied to a parasite. One problem is the antigen used to coat the dish. In the case of a virus, virions are effective antigens because a virus has relatively simple entry pathways mediated by a few surface molecules and the virion is soluble. By contrast, in the case of a parasite such as *Plasmodium falciparum*, which has multiple invasion pathways mediated by many ligands, an intact parasite itself cannot be used as the coating antigen. To solve this problem, we made a recombinant protein of interest fused with the Fc region of murine immunoglobulin G2a (mIgG2aFc). This protein can be coated on the bottom of a dish via an anti-mouse IgG Fc antibody.

The other problem is the criterion for selecting cells as the source of the cDNA library and target cells for an expression retrovirus cDNA library. For example, because the host cells of *P. falciparum* are erythrocytes that lack a nucleus, the construction of a cDNA library seems impossible. By contrast, because *Toxoplasma gondii* is thought to infect a broad host range of cells, it should be difficult to find cells that lack a receptor recognized by a *T. gondii* ligand. We attempted the following strategy to overcome this problem. The binding affinities between various cell types and the recombinant protein prepared as the coating were tested using flow cytometry. Cells with potent affinity were judged to have a receptor, whereas cells with weak or no affinity were judged to lack a receptor. Therefore, the former can serve as the source of the cDNA library and the latter can serve as target cells.

The procedure used in our modified method for screening for a parasite invasion receptor is shown in Fig. 1. To confirm whether this method works, we searched for a receptor for the *P. falciparum* protein BAEBL, which belongs to the Duffy binding-like family and is associated with erythrocyte invasion. Using a baculovirus expression system, region II of BAEBL, which is a critical region for binding, was expressed as a recombinant protein, designated BAEBL/Fc, fused with mIgG2aFc at the N terminal and an octa-histidine tag at the C terminal (Kobayashi et al., unpublished data). Similarly, a recombinant protein of the Fc region, designated

* Corresponding author. Fax: +81 3 5841 8184.
E-mail address: akkato@mail.ecc.u-tokyo.ac.jp (K. Kato).

[1] *Abbreviations used:* FIV, feline immunodeficiency virus; cDNA, complementary DNA; P3U1, P3S63Ag8U.1; PCR, polymerase chain reaction; mIgG2aFc, Fc region of murine immunoglobulin G2a; Tn5, BTI-Tn-5B1-4; Ni–NTA, nickel–nitrilotriacetic acid; mRNA, messenger RNA; MLV, Moloney murine leukemia virus; PBS, phosphate-buffered saline; 2FCS–PBS, PBS containing 2% fetal calf serum.

0003-2697/$ - see front matter © 2009 Elsevier Inc. All rights reserved.
doi:10.1016/j.ab.2009.03.008

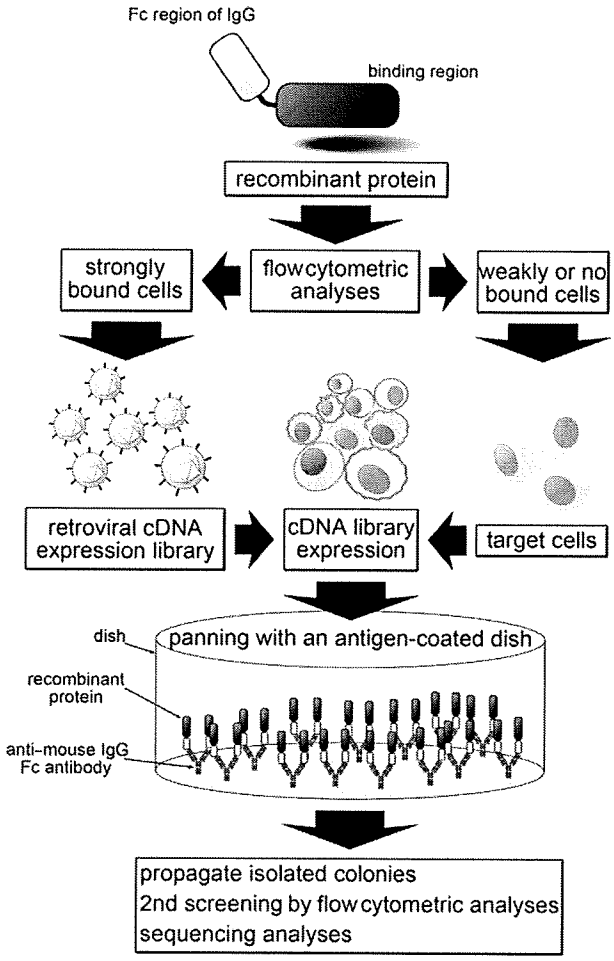

Fig. 1. Flow diagram of retrovirus-mediated expression cloning of a receptor recognized by a parasite. An Fc fusion protein containing the binding region of a molecule of interest is examined by testing its binding affinity to several cell lines. A retroviral cDNA library is constructed using mRNA extracted from cells showing strong binding affinity. Cells showing weak or no affinity are infected with a retrovirus stock carrying the cDNA library and then added to a dish coated with the recombinant protein and panned to isolate adhesive colonies. The colonies are subjected to flow cytometry to confirm the ligand binding. The cDNA sequences extracted from the confirmed cells are then analyzed.

mIgG2aFc, was prepared as a negative control. These proteins secreted from *Trichoplusia ni* BTI-Tn-5B1-4 (Tn5) insect cells were purified on nickel–nitrilotriacetic acid (Ni–NTA) agarose for flow cytometric analysis.

Next, we assessed the binding ability of BAEBL/Fc to several cell lines, including COS7, NIH3T3, P3U1, CrFK, FL74, 293T, Jurkat, and K562 cells, using flow cytometry. The cells (1×10^5) were resuspended in 27 nM purified recombinant protein solution and incubated for 1 h at 4 °C. The binding of the recombinant protein was detected using an anti-mouse IgG antibody labeled with fluorescein isothiocyanate, as described previously [4], and was quantified using FACSCalibur (Becton Dickinson, San Jose, CA, USA) and WinMDI 2.9 software. BAEBL/Fc showed relatively strong affinity for 293T human kidney cells and showed relatively weak affinity for Jurkat human T-cells (Fig. 2A and B), suggesting that 293T cells express a receptor for BAEBL.

A cDNA library was constructed using a previously described method [4,5] with several modifications. The cDNA library was generated from poly(A)+ messenger RNA (mRNA) purified from 293T cells and cloned into pMX. The cDNA library was packed into Moloney murine leukemia virus (MLV) particles by transfection into Plat-E cells and used to transduce Jurkat–EcoVRc cells. These are MLV-sensitive Jurkat cells that express the mouse cationic amino acid transporter and are prepared using a self-inactivating human immunodeficiency virus vector [7].

A dish was incubated at 4 °C overnight with 10 μg/ml goat anti-mouse IgG Fc (Rockland, Gilbertsville, PA, USA) in 4 ml of phosphate-buffered saline (PBS), rinsed in PBS containing 2% fetal calf serum (2FCS–PBS), and then incubated at room temperature for 30 min in 2FCS–PBS. The culture supernatant (10 ml) from Tn5 cells expressing BAEBL/Fc was added to the dish and incubated at room temperature for 30 min. The medium was replaced twice. The coated protein was fixed by incubating the dish in culture supernatant containing 1% paraformaldehyde at room temperature for 30 min. The dish was then washed five times in 2FCS–PBS before adding 1×10^7 transduced Jurkat–EcoVRc cells suspended in 4 ml of 2FCS–PBS. The cells were incubated at 37 °C for 2 h. Nonadherent cells were removed by washing. Adherent cells were cultured for 6 days, with a second wash on day 3. The adherent cells that formed colonies were suspended by pipetting in a penicillin cup and were transferred to a new culture plate. After propagating each clone, the reactivity of BAEBL against each clone was reconfirmed using flow cytometry. We obtained a clone, designated BJT6, to which BAEBL/Fc binds strongly (Fig. 2C). Genomic DNA from BJT6 was isolated and subjected to PCR amplification using KOD plus polymerase (Toyobo, Osaka, Japan) and the pMX primers [8]. Following amplification, this clone yielded a specific cDNA fragment encoding the full-length open reading frame of human glypican 1.

To confirm that glypican 1 really contributes to BAEBL binding, we evaluated the difference in the affinity of BAEBL/Fc to cells with or without glypican 1. Human glypican 1 cDNA was cloned into the *Bam*HI/*Sal*I sites of pMX to produce pMX–glypican 1. Jurkat–glypican 1 and Jurkat–mock cells were produced by the transfection of pMX–glypican 1 and pMX vectors, respectively, into Plat-E cells using Lipofectamine 2000 (Invitrogen, Carlsbad, CA, USA). Jurkat–EcoVRc cells were incubated with the culture supernatant from the transfected Plat-E cells and were analyzed 2 to 4 days postinfection. The flow cytometric analysis indicated that BAEBL/Fc showed greater affinity for Jurkat–glypican 1 than for Jurkat–mock (Fig. 2D and E), indicating that glypican 1 enhances the binding of BAEBL to the cell surface. This suggested that heparan sulfate proteoglycans, such as glypican 1, function to promote BAEBL binding and merozoite invasion, as seen in further analyses (Kobayashi et al., unpublished data). As shown here, this modified receptor screening strategy is applicable to parasite studies and has potential to increase our understanding of parasites.

Acknowledgments

This study was supported by a Grant-in-Aid for Young Scientists from the Ministry of Education, Culture, Sports, Science, and Technology (MEXT) of Japan and the Bio-oriented Technology Research Advancement Institution (BRAIN).

References

[1] T. Kitamura, M. Onishi, S. Kinoshita, A. Shibuya, A. Miyajima, G.P. Nolan, Efficient screening of retroviral cDNA expression libraries, Proc. Natl. Acad. Sci. USA 92 (1995) 9146–9150.
[2] M. Onishi, S. Kinoshita, Y. Morikawa, A. Shibuya, J. Phillips, L.L. Lanier, D.M. Gorman, G.P. Nolan, A. Miyajima, T. Kitamura, Applications of retrovirus-mediated expression cloning, Exp. Hematol. 24 (1996) 324–329.
[3] M. Shimojima, T. Miyazawa, Y. Sakurai, Y. Nishimura, Y. Tohya, Y. Matsuura, H. Akashi, Usage of myeloma and panning in retrovirus-mediated expression cloning, Anal. Biochem. 315 (2003) 138–140.
[4] M. Shimojima, T. Miyazawa, Y. Ikeda, E.L. McMonagle, H. Haining, H. Akashi, Y. Takeuchi, M.J. Hosie, B.J. Willett, Use of CD134 as a primary receptor by the feline immunodeficiency virus, Science 303 (2004) 1192–1195.
[5] A. Makino, M. Shimojima, T. Miyazawa, K. Kato, Y. Tohya, H. Akashi, Junctional adhesion molecule 1 is a functional receptor for feline calicivirus, J. Virol. 80 (2006) 4482–4490.

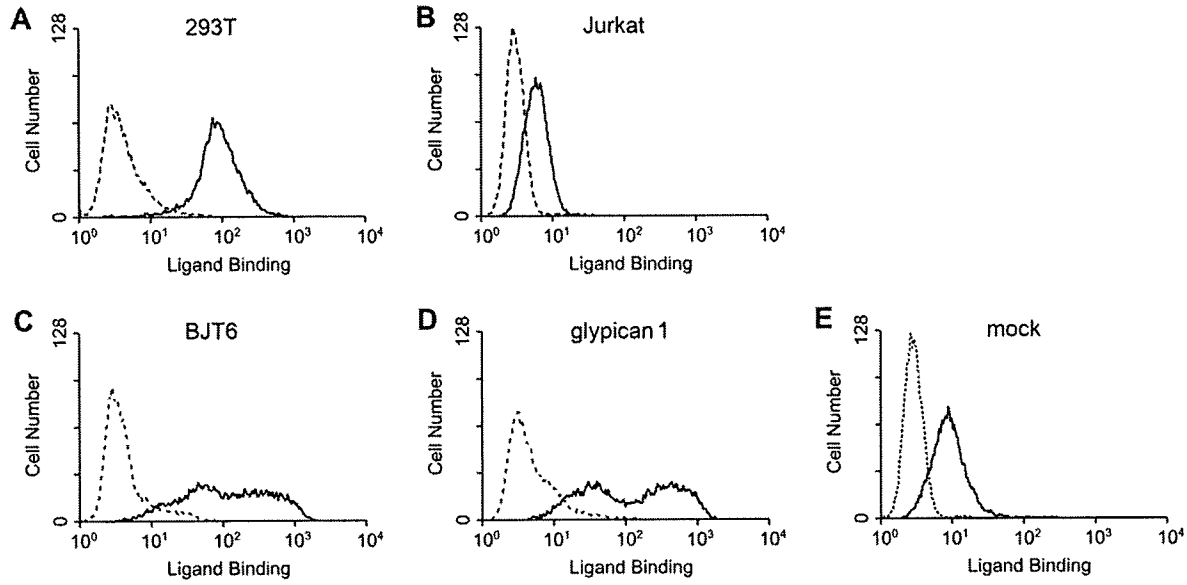

Fig. 2. Detection of recombinant protein binding using flow cytometry. The affinity of BAEBL/Fc (solid line) compared with mIgG2aFc (broken line) was determined for several cell lines. BAEBL/Fc bound strongly to 293T cells (A) and relatively poorly to Jurkat cells (B). The BJT6 clone was isolated as a result of the expression cloning (C). Jurkat–EcoVRc cells transduced with a retrovirus vector carrying cDNA of glypican 1 (D) or an empty plasmid (E) were incubated with BAEBL/Fc (solid line) or mIgG2aFc (broken line). Protein binding was detected and quantified as described in the text.

[6] T. Kitamura, Y. Koshino, F. Shibata, T. Oki, H. Nakajima, T. Nosaka, H. Kumagai, Retrovirus-mediated gene transfer and expression cloning: powerful tools in functional genomics, Exp. Hematol. 31 (2003) 1007–1014.

[7] M. Shimojima, Y. Ikeda, Y. Kawaoka, The mechanism of Axl-mediated Ebola virus infection, J. Infect. Dis. 196 (Suppl. 2) (2007) S259–S263.

[8] T. Kitamura, Y. Morikawa, Isolation of T-cell antigens by retrovirus-mediated expression cloning, Methods Mol. Biol. 134 (2000) 143–152.

JOURNAL OF VIROLOGY, May 2009, p. 4153–4162 Vol. 83, No. 9
0022-538X/09/$08.00+0 doi:10.1128/JVI.02642-08

Mutational Analysis of Conserved Amino Acids in the Influenza A Virus Nucleoprotein▽†

Zejun Li,[1] Tokiko Watanabe,[1] Masato Hatta,[1] Shinji Watanabe,[1] Asuka Nanbo,[1] Makoto Ozawa,[2] Satoshi Kakugawa,[2] Masayuki Shimojima,[2] Shinya Yamada,[2] Gabriele Neumann,[1] and Yoshihiro Kawaoka[1,2,3,4]*

Department of Pathobiological Sciences, School of Veterinary Medicine, University of Wisconsin—Madison, 2015 Linden Drive, Madison, Wisconsin 53706[1]; Division of Virology, Department of Microbiology and Immunology,[2] and International Research Center for Infectious Diseases, Institute of Medical Science,[3] University of Tokyo, Tokyo 108-8639, Japan; and ERATO Infection-Induced Host Responses Project, Japan Science and Technology Agency, Saitama 332-0012, Japan[4]

Received 22 December 2008/Accepted 10 February 2009

The nucleoprotein (NP), which has multiple functions during the virus life cycle, possesses regions that are highly conserved among influenza A, B, and C viruses. To better understand the roles of highly conserved NP amino acids in viral replication, we conducted a comprehensive mutational analysis. Using reverse genetics, we attempted to generate 74 viruses possessing mutations at conserved amino acids of NP. Of these, 48 mutant viruses were successfully rescued; 26 mutants were not viable, suggesting a critical role of the respective NP amino acids in viral replication. To identify the step(s) in the viral life cycle that is impaired by these NP mutations, we examined viral-genome replication/transcription, NP localization, and incorporation of viral-RNA segments into progeny virions. We identified 15 amino acid substitutions in NP that inhibited viral-genome replication and/or transcription, resulting in significant growth defects of viruses possessing these substitutions. We also found several NP mutations that affected the efficient incorporation of multiple viral-RNA (vRNA) segments into progeny virions even though a single vRNA segment was incorporated efficiently. The respective conserved amino acids in NP may thus be critical for the assembly and/or incorporation of sets of eight vRNA segments.

Influenza A virus consists of eight negative-sense single-stranded viral genomic-RNA segments and encodes at least 11 proteins (reviewed in reference 39). These genomic RNAs are incorporated into virions as ribonucleoprotein (RNP) complexes, which consist of the viral RNA (vRNA) associated with three viral polymerase subunit proteins (PA, PB1, and PB2) and nucleoprotein (NP). Upon binding to cell surface receptors, virions are internalized by receptor-mediated endocytosis. After fusion of the viral and endosomal membranes, the viral RNPs (vRNPs) are released into the cytoplasm and transported to the nucleus, where viral-genome replication and transcription take place (34). Newly synthesized vRNAs are associated with the NP and form vRNPs in the nucleus (4). Subsequently, the vRNPs are transported to the cytoplasm and packaged into the progeny virus particles, which then bud from the cells.

NP, a basic protein composed of 498 amino acids, is a major component of vRNPs (reviewed in reference 33). It contains an RNA-binding region at its N terminus (residues 1 to 181) (1, 19) and two domains, responsible for NP-NP self-interaction, at residues 189 to 358 and 371 to 465 (8) (Fig. 1A). Both of these NP functions are important to maintain the organization of vRNPs. Besides its structural role, NP is involved in many other functions throughout the virus replication cycle. In the early stages of the viral life cycle, NP facilitates vRNP import into the nucleus via its two nuclear localization signals (NLSs), an unconventional NLS (residues 3 to 13) and a bipartite NLS (residues 198 to 216) (35). NP also plays a role in RNA synthesis in the nucleus (15). It is required for the synthesis of longer RNAs, although three polymerase proteins are sufficient to synthesize short RNAs (14). NP also interacts with the viral polymerase proteins PB1 and PB2 (3), suggesting a potential role in the regulation of polymerase activity. Export of vRNPs from the nucleus to the cytoplasm is promoted via an interaction between NP and M1/NS2 (2, 22, 27, 29, 38, 40, 42). NP has an important role in RNP export; besides binding to the M1 protein, NP contains a cytoplasmic accumulation signal (residues 327 to 345), which interacts with F actin and causes cytoplasmic retention of NP late in infection (2, 5). In addition, NP contains a nuclear export signal that is recognized by the nuclear export receptor CRM1 (9). Overexpression of CRM1 biases transfected NP toward cytoplasmic accumulation, and the two proteins interact in in vitro binding assays (9).

The NP possesses regions that are highly conserved among influenza A, B, and C viruses (23). Mena et al. (23) used mutational analysis to identify several amino acid residues that are important for vRNA replication in the conserved regions of NP. For most of the conserved amino acids, however, the biological significance and the role in the viral life cycle remain unknown. To close this gap in knowledge, we attempted to generate 74 mutant viruses possessing mutations at conserved

* Corresponding author. Mailing address: Department of Pathobiological Sciences, School of Veterinary Medicine, University of Wisconsin—Madison, 2015 Linden Drive, Madison, WI 53706. Phone: (608) 265-4925. Fax: (608) 265-5622. E-mail: kawaokay@svm.vetmed.wisc.edu.

† Supplemental material for this article may be found at http://jvi.asm.org/.

▽ Published ahead of print on 18 February 2009.

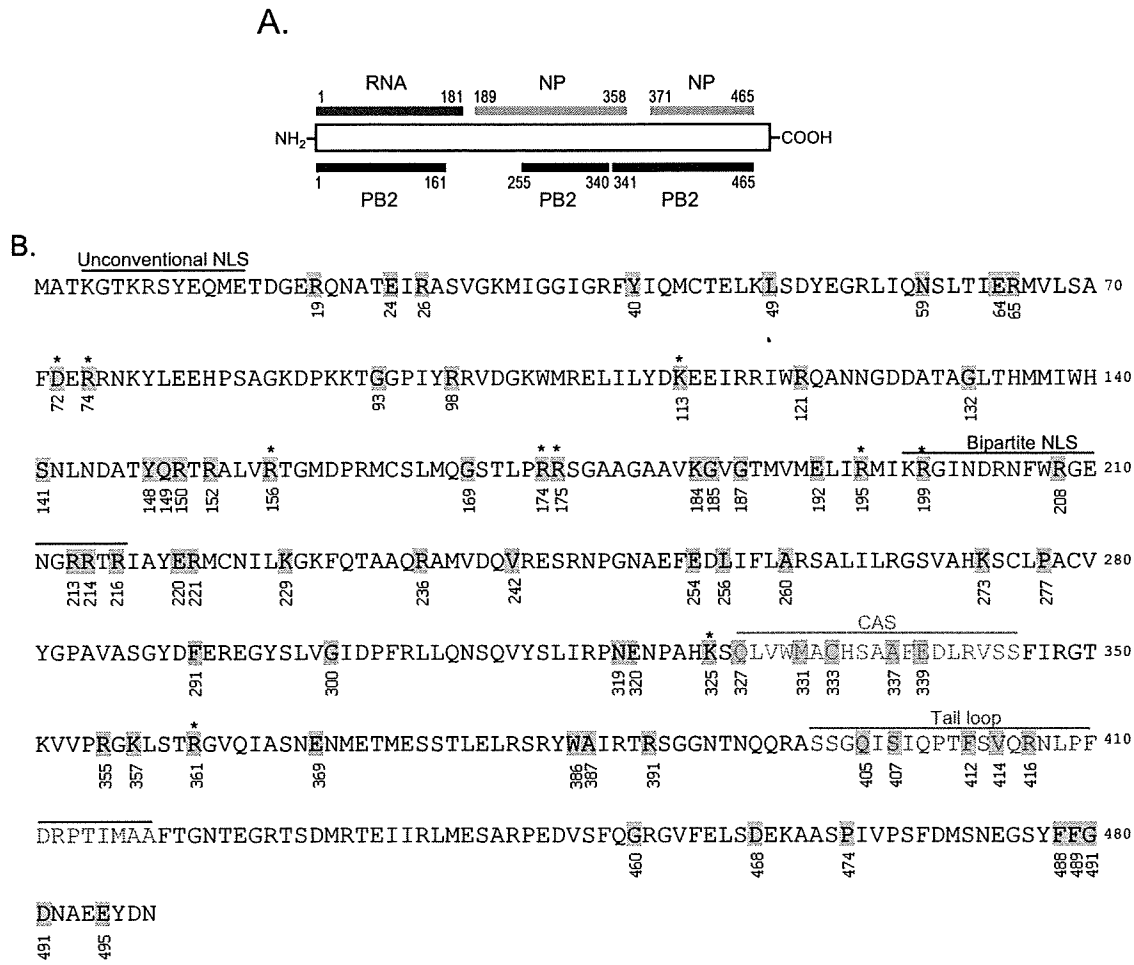

FIG. 1. Individual residues targeted by mutagenesis. (A) The NP regions responsible for binding to RNA (red), NP itself (orange), and PB2 (purple) are shown. (B) Amino acid sequence of WSN NP. Amino acids tested in this study are shaded. The unconventional NLS, the bipartite NLS, the cytoplasmic accumulation signal (CAS), and the NP tail loop, which mediates NP oligomerization, are shown in different colors. NP mutants flagged with an asterisk were further tested for intracellular localization and incorporation efficiency of a vRNA segment(s) into VLPs, in addition to replicative ability and polymerase activity.

residues of NP, and for the mutations that did not support viral growth, we studied the steps at which the mutations negatively affected NP functions.

MATERIALS AND METHODS

Cells. 293T cells were maintained in Dulbecco's modified Eagle medium supplemented with 10% fetal calf serum. Madin-Darby canine kidney (MDCK) cells were maintained in minimum essential medium containing 5% newborn calf serum. NP-expressing MDCK (MDCK-NP) cells were maintained in minimum essential medium containing 5% newborn calf serum and 5 μg/ml puromycin. All cells were maintained at 37°C in 5% CO_2.

MDCK-NP cells stably expressing NP from A/WSN/33 (H1N1; WSN) were established by infecting MDCK cells with retroviruses that were generated by cotransfecting 293T cells with the murine leukemia virus retroviral vector pMX (30) containing the NP gene, the internal ribosome entry site (IRES) sequence, and the puromycin resistance gene (designated pMX-WSNNP-IRES-puro [see below]) and plasmids expressing Gal/Pol, NF-κB, and vesicular stomatitis virus G protein (17), which were kind gifts from Bill Sugden (University of Wisconsin—Madison). A stable MDCK cell clone expressing NP was selected in medium containing 0.15 mg/ml puromycin (Roche, Mannheim, Germany) by indirect immunostaining with a monoclonal antibody to NP.

Plasmid construction. The NP segment of WSN virus was reverse transcribed with an oligonucleotide complementary to the conserved 3′ end of the vRNA (16) and a pair of NP gene-specific oligonucleotide primers containing BsmBI sites. The PCR product was cloned into the pT7Blueblunt vector (Novagen, Madison, WI), and the resultant plasmid was referred to as pT7-WSN-NP. After digestion with BsmBI, the fragment containing the NP gene was cloned into the BsmBI sites of the pHH21 vector, which contains the human RNA polymerase I promoter and the mouse RNA polymerase I terminator separated by BsmBI sites (24), resulting in the generation of pPolI-NP (all plasmids derived from pHH21 for the expression of vRNA are referred to as PolI constructs in this report).

pCAGGs/MCS-NP, for the expression of the NP protein, was generated by inserting the BsmBI-digested NP fragment into the BsmBI sites of a modified pCAGGS/MCS (18, 25) vector. The substitution mutations listed in Table 1 were first introduced into the pT7-WSN-NP plasmid by in vitro site-directed mutagenesis (Stratagene, La Jolla, CA) and then subcloned into the pHH21 and pCAGGS/MCS vectors by using the unique BsmBI restriction enzyme sites. All mutations were verified by sequencing.

pPolI-WSN-NA-*firefly*-luciferase produces a virus-like RNA in which the coding region for firefly luciferase is flanked by the packaging signals of the NA segment (12). This plasmid was generated by inserting the firefly luciferase open reading frame between the BamHI and XhoI sites of pPolI-WSN-NA-MCS, which was constructed by modifying the start codon of pPolINA(183)GFP(157) (12) (in essence, we replaced ATATG at nucleotide positions 113 to 117 and 161 to 165 with GCGCG) and by replacing the sequence from the initiation of the enhanced green fluorescent protein (GFP) gene to the StuI site on pPolI-WSN-NA(183)GFP(157). pPolI-HA-GFP, for the generation of a virus-like RNA encoding GFP, was generated as described previously (36).

pCAGGS-*Renilla*, for the expression of *Renilla* luciferase, was generated by

TABLE 1. Phenotypic analyses of mutant NP proteins

NP[a]	Virus rescue[b]	Mean virus titer at 48 h postinfection (log_{10} PFU/ml) ±SD[c]		Group[d]	Relative luciferase activity at 48 h posttransfection (%)[e]	
		33°C	37°C		33°C	37°C
Wild type	+	7.99 ± 0.01	8.85 ± 0.07	I	100.00 ± 6.88	100.00 ± 13.51
R19A	+	7.28 ± 0.02	9.00 ± 0.00	I	94.68 ± 4.14	88.26 ± 1.30
E24A	+	6.65 ± 0.05	8.67 ± 0.05	I	131.38 ± 14.44	95.84 ± 4.20
Y40A	+	7.98 ± 0.05	8.41 ± 0.01	I	91.83 ± 4.06	81.73 ± 5.45
L49A	+	8.12 ± 0.01	8.54 ± 0.07	I	151.00 ± 7.27	142.78 ± 8.76
R65A	+	6.29 ± 0.07	8.49 ± 0.02	I	138.46 ± 3.43	108.60 ± 17.82
R98A	+	8.30 ± 0.01	8.55 ± 0.06	I	108.01 ± 1.14	89.65 ± 3.67
R121A	+	6.37 ± 0.20	7.94 ± 0.02	I	144.83 ± 4.15	104.00 ± 2.76
G132A	+	7.62 ± 0.05	9.11 ± 0.02	I	145.46 ± 10.02	106.67 ± 4.86
S141A	+	8.09 ± 0.01	8.87 ± 0.05	I	133.72 ± 2.09	100.26 ± 3.02
Q149A	+	3.65 ± 0.01	7.51 ± 0.16	I	135.63 ± 6.60	102.19 ± 2.52
G169A	+	7.89 ± 0.03	8.43 ± 0.21	I	126.76 ± 2.21	94.92 ± 3.96
K184A	+	6.40 ± 0.08	7.68 ± 0.02	I	145.34 ± 11.35	96.27 ± 5.72
G185A	+	6.58 ± 0.16	7.46 ± 0.06	I	153.55 ± 6.32	95.09 ± 4.86
G187A	+	6.31 ± 0.23	8.43 ± 0.01	I	114.82 ± 5.33	99.31 ± 1.40
R214A	+	7.21 ± 0.01	8.01 ± 0.07	I	122.85 ± 4.95	87.02 ± 14.18
R216A	+	6.32 ± 0.06	6.92 ± 0.04	I	111.38 ± 4.64	85.36 ± 6.68
E220A	+	5.22 ± 0.06	8.57 ± 0.19	I	62.84 ± 3.39	103.46 ± 8.18
K229A	+	6.92 ± 0.01	8.03 ± 0.09	I	113.40 ± 0.68	97.47 ± 5.12
R236A	+	5.07 ± 0.05	7.61 ± 0.00	I	107.59 ± 2.69	90.13 ± 14.06
V242A	+	7.67 ± 0.13	8.15 ± 0.11	I	136.01 ± 4.81	101.33 ± 2.46
L256A	+	6.33 ± 0.10	6.97 ± 0.07	I	143.86 ± 3.42	87.44 ± 1.70
P277A	+	8.31 ± 0.01	8.79 ± 0.03	I	131.35 ± 3.02	98.03 ± 2.96
F291A	+	7.15 ± 0.05	8.41 ± 0.01	I	126.04 ± 3.53	89.44 ± 5.27
G300A	+	5.02 ± 0.06	7.75 ± 0.01	I	100.10 ± 3.52	86.88 ± 3.82
N319A	+	7.75 ± 0.11	8.36 ± 0.05	I	107.45 ± 2.23	81.28 ± 4.23
Q327A	+	6.74 ± 0.09	7.19 ± 0.27	I	125.66 ± 0.88	95.25 ± 7.13
C333A	+	8.06 ± 0.05	8.9 ± 0.01	I	105.19 ± 4.78	99.49 ± 6.63
K357A	+	7.78 ± 0.01	8.7 ± 0.08	I	105.22 ± 0.25	81.12 ± 1.17
E369A	+	7.27 ± 0.21	7.98 ± 0.02	I	114.80 ± 4.74	142.64 ± 1.72
W386A	+	5.44 ± 0.11	7.53 ± 0.05	I	88.39 ± 4.83	125.05 ± 8.59
G460A	+	6.68 ± 0.06	8.88 ± 0.04	I	118.59 ± 17.56	138.93 ± 10.31
P474A	+	6.04 ± 0.03	8.79 ± 0.08	I	115.52 ± 3.98	116.35 ± 3.24
G490A	+	7.63 ± 0.04	8.86 ± 0.13	I	113.78 ± 11.54	104.90 ± 6.71
E495A	+	7.21 ± 0.09	8.3 ± 0.02	I	73.02 ± 1.39	83.08 ± 7.90
R26A	+	1.54 ± 0.09	3.81 ± 0.03	II	79.44 ± 0.71	85.62 ± 1.65
*R74A	+	3.11 ± 0.09	4.42 ± 0.08	II	139.73 ± 9.61	109.25 ± 2.07
*R175A	+	2.91 ± 0.01	4.11 ± 0.05	II	170.32 ± 5.96	108.56 ± 6.54
E192A	+	4.16 ± 0.02	6.03 ± 0.01	II	78.03 ± 3.16	82.87 ± 1.66
R221A	+	4.56 ± 0.03	4.75 ± 0.13	II	111.94 ± 4.57	93.17 ± 4.51
M331A	+	1.00 ± 0.00	4.77 ± 0.1	II	99.45 ± 8.38	83.98 ± 7.56
R391A	+	2.89 ± 0.03	6.57 ± 0.02	II	70.66 ± 2.04	63.56 ± 0.46
S407A	+	1.00 ± 0.00	6.19 ± 0.03	II	5.40 ± 0.39	86.15 ± 0.28
V414A	+	1.69 ± 0.12	6.85 ± 0.06	II	47.29 ± 6.11	92.27 ± 1.14
D468A	+	3.54 ± 0.34	6.67 ± 0.10	II	97.46 ± 2.33	81.45 ± 5.87
D491A	+	5.09 ± 0.07	5.82 ± 0.09	II	52.09 ± 0.67	73.18 ± 4.46
N59A	+	ND	ND	III	159.52 ± 4.80	54.32 ± 1.72
E64A	+	ND	ND	III	193.40 ± 14.30	0.03 ± 0.00
E320A	+	ND	ND	III	145.78 ± 6.37	51.05 ± 1.47
*D72A	−	ND	ND	IV	121.17 ± 1.30	135.07 ± 1.05
G93A	−	ND	ND	IV	131.30 ± 10.53	55.13 ± 2.74
*K113A	−	ND	ND	IV	183.46 ± 12.21	106.16 ± 5.07
Y148A	−	ND	ND	IV	100.87 ± 3.15	82.89 ± 10.15
R150A	−	ND	ND	IV	12.46 ± 0.79	32.17 ± 1.44
R152A	−	ND	ND	IV	100.52 ± 1.78	77.61 ± 14.19
*R156A	−	ND	ND	IV	123.85 ± 6.03	95.24 ± 3.16
*R174A	−	ND	ND	IV	214.89 ± 17.15	100.56 ± 6.91
*R195A	−	ND	ND	IV	160.59 ± 14.23	105.41 ± 5.63
*R199A	−	ND	ND	IV	152.91 ± 10.97	102.41 ± 6.38
R208A	−	ND	ND	IV	0.19 ± 0.01	0.13 ± 0.01
R213A	−	ND	ND	IV	32.42 ± 0.36	38.29 ± 7.36
E254A	−	ND	ND	IV	0.26 ± 0.03	0.37 ± 0.13
A260R	−	ND	ND	IV	0.04 ± 0.00	0.02 ± 0.01
K273A	−	ND	ND	IV	0.19 ± 0.02	0.04 ± 0.01
*K325A	−	ND	ND	IV	157.38 ± 7.37	134.67 ± 12.73

Continued on following page

TABLE 1—*Continued*

NP[a]	Virus rescue[b]	Mean virus titer at 48 h postinfection (log_{10} PFU/ml) ±SD[c]		Group[d]	Relative luciferase activity at 48 h posttransfection (%)[e]	
		33°C	37°C		33°C	37°C
A337R	−	ND	ND	IV	0.16 ± 0.00	0.03 ± 0.00
E339A	−	ND	ND	IV	0.16 ± 0.01	0.03 ± 0.01
R355A	−	ND	ND	IV	52.91 ± 0.47	45.07 ± 1.06
*R361A	−	ND	ND	IV	105.57 ± 0.49	104.60 ± 20.58
A387R	−	ND	ND	IV	0.15 ± 0.00	0.04 ± 0.00
Q405A	−	ND	ND	IV	0.16 ± 0.01	0.05 ± 0.01
F412A	−	ND	ND	IV	0.40 ± 0.32	0.03 ± 0.00
R416A	−	ND	ND	IV	0.21 ± 0.10	0.03 ± 0.00
F488A	−	ND	ND	IV	0.20 ± 0.01	8.05 ± 1.02
F489A	−	ND	ND	IV	0.16 ± 0.01	0.23 ± 0.22

[a] We selected 74 amino acids that are conserved among influenza A, B, and C virus NPs for mutagenesis. NP mutants flagged with an asterisk were further tested for intracellular localization, and incorporation efficiency of a vRNA segment(s) into VLPs, in addition to replicative ability and polymerase activity.

[b] Viruses were generated using an established plasmid-based reverse-genetics system. +, NP mutant virus recovery was verified by plaque assay, cytopathic effect, and NP gene sequencing; −, no replicating virus was recovered.

[c] MDCK cells were infected with wild-type WSN or NP mutant virus at an MOI of 0.0001. At 48 h postinfection, the culture supernatants were harvested and subjected to plaque assays in MDCK cells. ND, plaques were not detected.

[d] Based on virus rescue and viral-replication properties, NP mutants were categorized into four groups. Group I, at either 33°C or 37°C, viruses were attenuated by less than 2 log units; group II, mutant viruses were attenuated by more than 2 log units at both temperatures tested; group III, NP mutant viruses were rescued but did not form plaques at 48 h postinfection; group IV, NP mutant virus were not rescued.

[e] The abilities of mutant NPs to support vRNA replication/transcription in an in vitro assay were examined in 293T cells as described in Materials and Methods. Since luciferase levels reflect the overall transcription and replication activity of the polymerase complex, we defined the polymerase activity levels as high, normal, and low for mutants that exhibited >120%, 80% to 120%, and <80%, respectively, of the wild-type activity.

inserting the open reading frame of the *Renilla* luciferase gene into the BsmBI sites of pCAGGs/MCS.

The pPolI-NP(Met$^-$) plasmid, used to generate vRNA that did not encode NP due to the lack of a start codon, was generated by changing the 1st through the 7th ATG codons to TAG and by changing the 14th and 15th ATG codons to TAG and TGA, respectively, using in vitro site-directed mutagenesis (Stratagene, La Jolla, CA).

The plasmid pMX-WSNNP-IRES-puro was constructed as follows. First, the puromycin resistance gene was inserted into XbaI and SalI sites of the plasmid pIRES (Clontech, Mountain View, CA), and then a fragment containing the IRES sequence and the puromycin resistance gene was inserted into EcoRI and SalI sites of the pMX retroviral vector (30). This plasmid was designated pMX-IRES-puro. Finally, the WSN NP gene was cloned into EcoRI and MluI sites of pMX-IRES-puro.

Plasmid-driven reverse genetics. All viruses used in this study were generated by reverse genetics, using plasmids expressing the eight vRNA segments, the three polymerase proteins, and NP, as described by Neumann et al. (24). At 48 h posttransfection, viruses were harvested and used to inoculate MDCK cells for the production of stock viruses. The NP genes of transfectant viruses were sequenced to confirm the origins of the genes and the presence of the intended mutations and to ensure that no unwanted mutations were present.

Virus-like particles (VLPs) were generated from 293T cells transfected with eight PolI constructs producing eight vRNA segments [i.e., PB1, PB2, PA, NA, M, NS, HA-GFP, and NP(Met$^-$), which lacks a start codon] and five protein expression constructs producing PB1, PB2, PA, hemagglutinin (HA), and mutant or wild-type NP (see Fig. 3). These plasmids were mixed with transfection reagent (2 μl of Trans IT LT-1 [Mirus, Madison, WI] per μg of DNA), incubated at room temperature for 20 min, and added to 10^6 293T cells. Six hours later, the DNA transfection reagent mixture was replaced by 1 ml Opti-MEM (Invitrogen, Grand Island, NY). Forty-eight hours after transfection, the supernatant was harvested, treated with trypsin, and used to determine the number of VLPs containing the test genes, as described below.

Replicative properties of viruses. MDCK cells were infected with wild-type WSN or NP mutant virus at a multiplicity of infection (MOI) of 0.0001 at 33°C and 37°C, respectively. At 48 h postinfection, the culture supernatants were collected and subjected to plaque assays in MDCK cells for virus titration.

Luciferase assay. 293T cells were transfected with plasmids for the expression of the viral proteins PA, PB1, PB2, and NP (wild-type or mutated NP) and pPolI-WSN-NA-*firefly*-luciferase. Plasmid pCAGGS-*Renilla* was used as an internal control for the dual-luciferase assay. As a negative control, 293T cells were transfected with the same plasmids, with the exception of the NP expression plasmid. After transfection, the cells were incubated at 33°C or 37°C for 48 h, and then luciferase activity was measured with a dual-luciferase reporter system (Promega, Madison, WI) on a Glomax microplate luminometer (Promega, Madison, WI) according to the manufacturer's instructions.

Immunostaining assay. MDCK cells were transfected with pCAGGs/MCS plasmids expressing wild-type or mutant NP. At 9 h and 24 h posttransfection, the cells were fixed and indirect immunofluorescence assays were performed. Briefly, the cells were washed twice with phosphate-buffered saline (PBS), fixed with 3.7% paraformaldehyde (in PBS) for 20 min at room temperature, washed again, and permeabilized with 0.5% Triton X-100 for 10 min. After being blocked with 10% bovine serum albumin for 20 min at room temperature, the cells were incubated with an anti-NP monoclonal antibody (347/3) for 30 min. The cells were then incubated with fluorescein isothiocyanate-labeled goat anti-mouse antibody immunoglobulin G (1:200 dilution; Roche) for 30 min, washed, and mounted with 10 mM *p*-phenylenediamine in glycerol-PBS (9:1), pH 8.5. To avoid the detection of newly synthesized NP, protein synthesis was inhibited by adding cycloheximide (50 mg/ml; Sigma) to the growth medium at 9 h posttransfection. Twenty-four hours later, indirect immunofluorescence assays were performed. Samples were observed under a fluorescence microscope or a confocal laser microscope (LSM510META; Carl Zeiss, Jena, Germany).

Determination of the number of VLPs. To determine the number of VLPs containing at least one vRNA (i.e., HA-GFP vRNA), culture supernatants of 293T cells transfected with plasmids for VLP production (as described above) were used to infect MDCK cells. To provide polymerase and NP that supported HA-GFP vRNA replication and transcription, cells were coinfected with WSN virus at an MOI of 0.1 (see Fig. 3). Sixteen hours postinfection, the infected cells were fixed, and the cells expressing GFP were counted under a fluorescence microscope.

To determine the number of VLPs containing a set of four vRNAs (i.e., PB1, PB2, PA, and HA-GFP vRNAs), the culture supernatants of transfected cells were used to infect MDCK-NP cells that stably expressed WSN NP (see Fig. 3). GFP expression from the HA-GFP vRNA would occur only if VLPs contained the HA-GFP vRNA together with the PB2, PB1, and PA vRNAs. GFP-positive cells, therefore, represented VLPs that possessed at least the PB2, PB1, PA, and HA-GFP vRNAs. As described above, the number of GFP-expressing cells was determined at 16 h postinfection.

RESULTS

Generation of NP mutant viruses. For mutagenesis, we selected amino acids that are highly conserved among influenza A, B, and C viruses, as well as amino acids that may be critical for RNA binding, as suggested by the recently published crystal

structure of influenza A virus NP (41). In total, 74 amino acid residues were selected for testing (Fig. 1B). Using plasmid-driven reverse genetics (24), we were able to generate 48 mutant viruses (Table 1). The remaining 26 mutant viruses were not viable (Table 1), suggesting that the respective mutations in NP are critical for the viral life cycle.

Replicative properties of NP mutant viruses. For all viable mutant viruses, we next examined their replicative abilities in cell culture. Briefly, MDCK cells were infected with wild-type WSN or NP mutant viruses at an MOI of 0.0001 and incubated at 33°C and 37°C. Forty-eight hours later, the culture supernatants were harvested and subjected to plaque assays in MDCK cells for virus titration. Based on their abilities to support viral replication, the NP mutants could be divided into four groups. As shown in Table 1, groups I, II, and III include all 48 recovered NP mutant viruses, while group IV contains the 26 nonviable mutant viruses.

Group I contains 34 mutant viruses whose titers were less than 2 log units lower than that of wild-type WSN virus at either 33°C or 37°C. Seventeen viruses (possessing NP mutations R19A, Y40A, L49A, R98A, G132A, S141A, G169A, R214A, V242A, P277A, F291A, N319A, C333A, K357A, E369A, G490A, and E495A) were attenuated by less than 1 log unit at both 33°C and 37°C. Mutant viruses Q149A, K184A, G185A, R216A, R236A, L256A, G300A, Q327A, and W386A were clearly attenuated at both 33°C and 37°C, with virus titers reduced by more than 1 log unit compared to wild-type WSN virus, whereas E24A, R65A, R121A, G187A, E220A, K229A, G460A, and P474A were attenuated only at 33°C. Of these viruses, mutants Q149A, E220A, R236A, G300A, and W386A were attenuated by more than 2.5 log units at 33°C. The NP sequences of these mutant viruses were reconfirmed, and one unexpected mutation was found at position 140 (His to Arg) in the NP protein of mutant R65A (the significance of this substitution is currently unknown).

The NP mutant viruses in group II were significantly attenuated, i.e., their titers were more than 2 log units lower than that of wild-type WSN virus at both 33°C and 37°C. Eleven NP mutant viruses (R26A, R74A, R175A, E192A, R221A, M331A, R391A, S407A, V414A, D468A, and D491A) comprised this group. The titers of four mutants (R26A, R74A, R175A, and M331A) were more than 4 log units lower than that of wild-type WSN virus at both 33°C and 37°C. Four other viruses (R391A, S407A, V414 A, and D468A) were attenuated by more than 4 log units at 33°C but only 2 to 3 log units at 37°C.

Group III contains three mutant viruses, N59A, E64A, and E320A, which were unable to form plaques, although cytopathic effects were observed in MDCK cells infected with these mutants. The 50% tissue culture infective doses of N59A, E64A, and E320A were 5.5, 3.5, and 6.5 $\log_{10}$ 50% tissue culture infective doses/ml at 33°C, respectively.

Group IV includes the 26 nonviable mutants (D72A, G93A, K113A, Y148A, R150A, R152A, R156A, R174A, R195A, R199A, R208A, R213A, E254A, A260R, K273R, K325A, A337R, E339R, R355A, R361A, R387A, Q405A, F412A, R416A, F488A, and F489A), attesting to a critical role of these amino acids in the viral life cycle.

Polymerase activities of replication complexes containing NP mutants. As stated above and shown in Table 1, we identified NP amino acid substitutions that caused viral growth defects. To assess the effects of these substitutions on vRNA transcription activity, we tested the activities of NP mutants by using a minireplicon system. pPolI-WSN-NA-*firefly*-luciferase synthesizes a modified influenza virus NA vRNA in which the coding region for firefly luciferase replaces the native NA coding sequences. The luciferase levels thus reflect the overall transcription and replication activities of the polymerase complex upon cotransfection of cells with pPolI-WSN-NA-*firefly*-luciferase and plasmids for the expression of the viral PA, PB1, PB2, and NP (wild-type or mutant NP), which support both replication and transcription from a vRNA template (32). At 48 h posttransfection, luciferase activity was measured. We found that NP mutants in group I, whose mutations had no or moderate effects on virus replicative ability, had at least 80% and 60% of the luciferase activity of wild-type NP at 37°C and 33°C, respectively (Table 1). NP mutant E220A showed reduced activity to support polymerase function at 33°C but not at 37°C. Other mutants in group I (i.e., Q149A, R236A, and G300A) showed no defect in supporting polymerase function compared to wild-type NP at 33°C, even though the respective virus titers were more than 2 log units lower than that of wild-type WSN virus at 33°C. Hence, these NP mutations do not affect genome replication and transcription, but other steps in the viral life cycle.

In group II, six NP mutants, R26A, E192A, R391A, S407A, V414A, and D491A, showed lower activity to support polymerase function at 33°C than wild-type NP, suggesting that these mutations may cause virus attenuation at low temperatures. Interestingly, R74A and R175A showed normal activity to support polymerase function at 37°C, and even higher activity at 33°C, compared to wild-type NP, whereas the respective viruses were attenuated by more than 4 log units. These results suggest that these mutations may inhibit steps other than genome replication and transcription, such as transport, assembly, and/or virion incorporation.

Mutants in group III showed some temperature sensitivity, expressing more than 145% of wild-type luciferase activity at 33°C but less than 55% at 37°C. Specifically, mutant E64A lost the ability to support reporter gene transcription at 37°C but expressed 193% of wild-type luciferase activity at 33°C. Notably, these mutant viruses could not form plaques at either 33°C or 37°C, even though they expressed higher luciferase activity than wild-type WSN virus at 33°C.

In group IV, many of the variants (i.e., R150A, R208A, R213A, E254A, A260R, K273A, A337R, E339A, R355A, A387R, Q405A, F412A, R416A, F488A, and F489A) showed no or very low luciferase activity at both 33°C and 37°C. Hence, these mutations likely lost the ability to support viral polymerase activity, resulting in the growth defect of the mutant viruses (Table 1). The remaining mutants expressed reasonable levels of luciferase activity at either 33°C or 37°C. Of these mutants, D72A, K113A, R156A, R174A, R195A, R199A, K325A, and R361A showed normal or high polymerase activity at both 33°C and 37°C despite the observed failure of virus rescue (Table 1). These data suggest a role of the respective amino acids in processes such as intracellular transport, assembly, and/or packaging.

Localization of mutant NPs. We found that 10 NP variants (D72A, R74A, K113A, R156A, R174A, R175A, R195A, R199A, K325A, and R361A) caused viral growth defects with no ap-

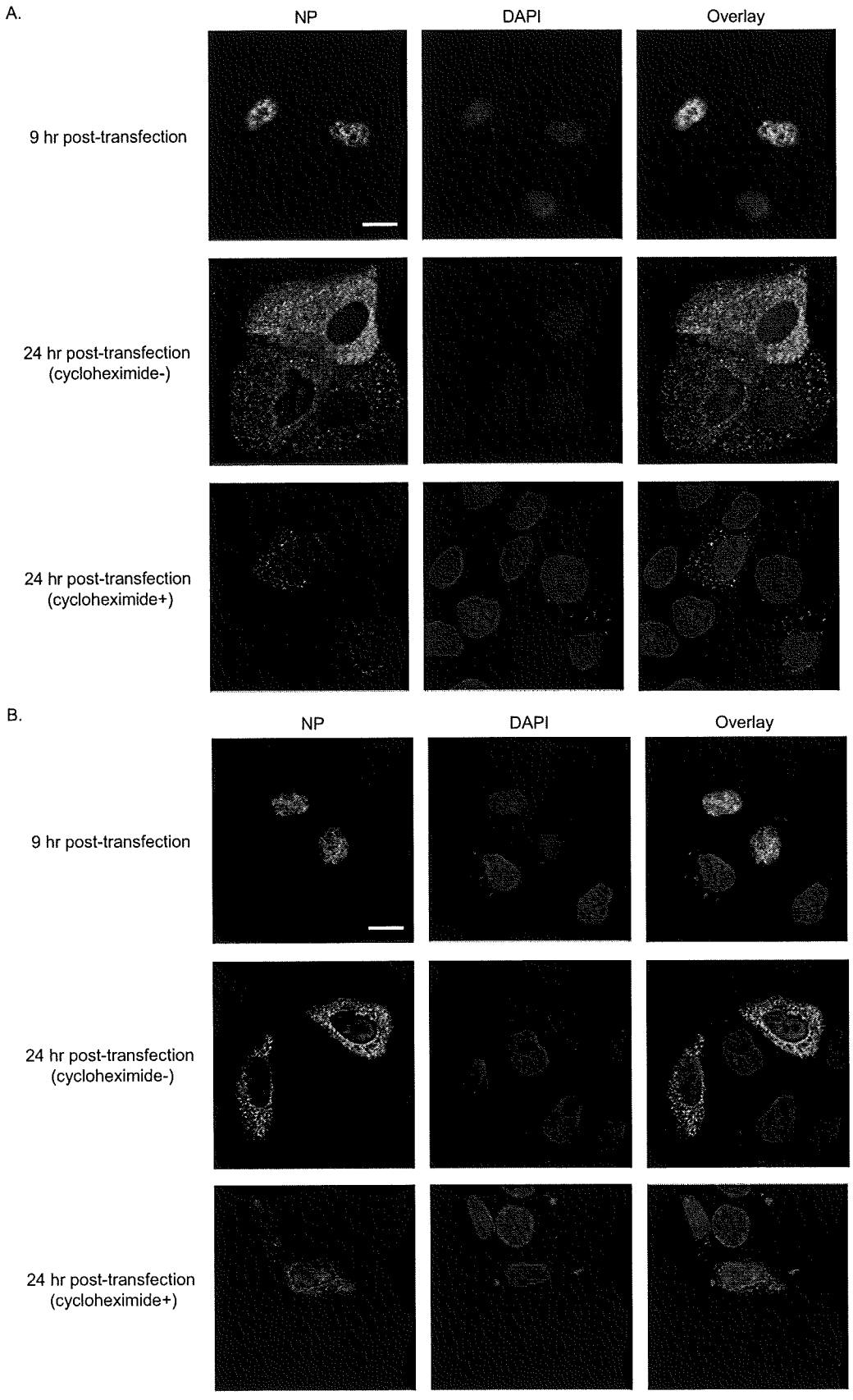

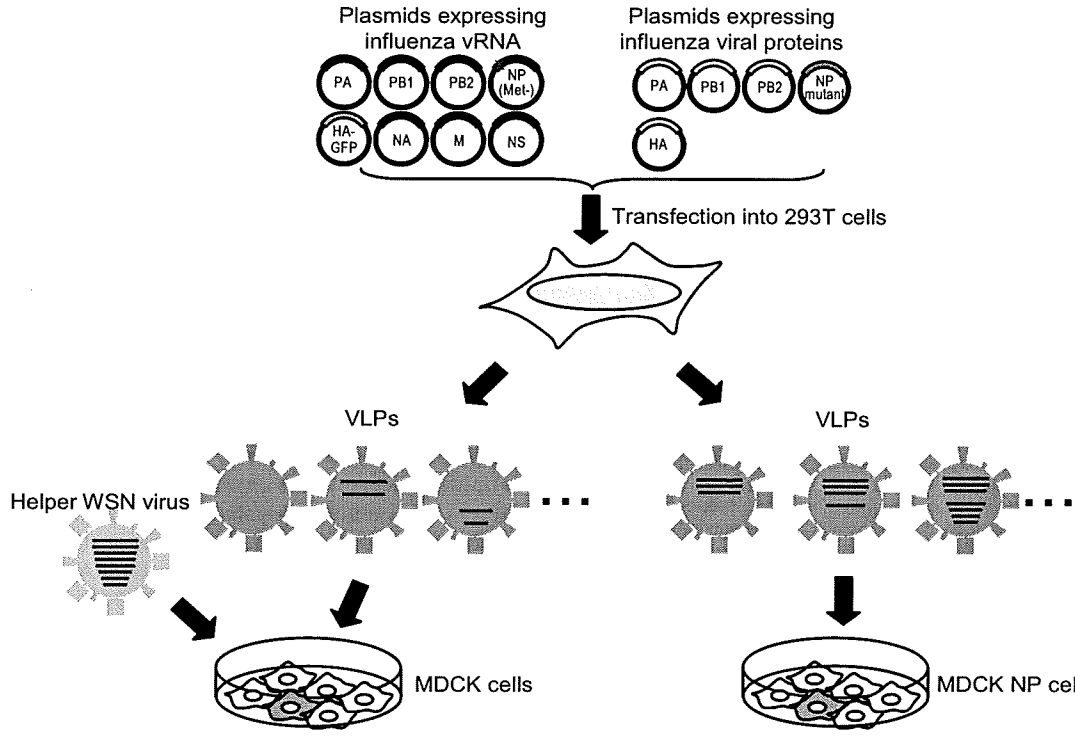

FIG. 3. System to test vRNP virion incorporation efficiencies. VLPs were recovered from 293T cells transfected with eight PolI constructs for the eight RNA segments PB1, PB2, PA, NA, M, NS, HA-GFP, and NP(Met$^-$), which lacks a start codon. These VLPs were used to infect MDCK cells in the presence of helper virus (left). In this experimental setting, GFP-positive MDCK cells are representative of VLPs that contain at least one vRNA segment (i.e., the HA-GFP vRNA). In a parallel experiment, VLPs derived from 293T cells were used to infect MDCK cells expressing NP (right). In this experimental setting, GFP-positive MDCK cells are indicative of VLPs that possess at least four vRNAs (i.e., the PB2, PB1, PA, and HA-GFP vRNAs).

parent effect on genome replication and transcription. For these variants, therefore, we assessed intracellular localization. MDCK cells were transfected with plasmids expressing mutant NPs, and indirect immunofluorescence assays were performed 9 h and 24 h after transfection. As shown in Fig. 2A and B and Fig. S1 in the supplemental material, 9 hours after transfection, wild-type NP and all NP mutants tested localized to the nuclei of transfected MDCK cells. Twenty-four hours after transfection, wild-type NP and all variants tested localized both to the nucleus and to the cytoplasm regardless of the addition of a translation inhibitor, cycloheximide. Since the localization of these mutant NPs was indistinguishable from that of the wild-type NP, their attenuated growth properties cannot be explained by defects in nuclear export.

Incorporation efficiency of a single vRNA segment into VLPs containing mutant NPs. For some NP mutants, the growth defects of the corresponding viruses cannot be explained by deficiencies in replication or intracellular transport. Therefore, we next examined the effects of the respective mutations on virus assembly. To determine the incorporation efficiency of vRNA segments into VLPs, we transfected 293T cells with eight PolI plasmids for the PB1, PB2, PA, NA, M, NS, HA-GFP, and NP(Met$^-$) vRNA segments. The NP(Met$^-$) vRNA produced an NP gene whose start codon was replaced with a stop codon to avoid expression of wild-type NP; the HA-GFP vRNA encodes the GFP reporter flanked by the packaging signals of the HA segment (36). Cells were cotransfected with five protein expression plasmids for PB1, PB2, PA, HA, and mutant or wild-type NP. The resultant VLPs were replication incompetent because they possessed mutant HA and NP vRNA segments instead of wild-type HA and NP vRNAs (Fig. 3). The supernatants of transfected cells were harvested at 48 h posttransfection and used to infect MDCK cells, together with a helper virus to provide a functional polymerase complex that supports the replication/transcription of HA-GFP vRNA. The number of VLPs containing the HA-GFP vRNA segment was

FIG. 2. Localization of NP mutants. MDCK cells transfected with plasmids expressing mutant NP or wild-type NP were subjected to indirect immunofluorescence assays. NP and DNA were stained with an anti-NP antibody and DAPI (4′,6′-diamidino-2-phenylindole), respectively. Samples were observed under a confocal laser microscope. Nine hours after transfection, wild-type and mutant NP exclusively localized to the nucleus. Shown are wild-type NP (A) and mutant R175A as a representative example of the mutants tested (B). Twenty-four hours after transfection, wild-type NP and all mutant NPs tested localized to both the nucleus and the cytoplasm, regardless of the addition of the translational inhibitor cycloheximide at 9 h posttransfection. The localization of the mutant NP proteins was indistinguishable from that of wild-type NP. Scale bars, 20 μm.

TABLE 2. Virion incorporation efficiencies of vRNA segments[a]

NP	No. of VLPs possessing at least one vRNA (per ml)[b]	No. of VLPs possessing at least four vRNAs (per ml)[c]
Wild type	31,900	17,800
D72A	450	0
R74A	62,500	390
K113A	2,160	0
R156A	167,000	11
R174A	8,980	0
R175A	100,000	0
R195A	26,200	0
R199A	51,000	0
K325A	5,700	0
R361A	21,080	0

[a] 293T cells were transfected with eight PolI constructs for eight RNA segments [i.e., PB1, PB2, PA, NA, M, NS, HA-GFP, and NP(Met$^-$), which lacks a start codon] and five protein expression constructs for PB1, PB2, PA, HA, and mutant or wild-type NP. Forty-eight hours later, VLPs were harvested, treated with TPCK trypsin, and used to determine the virion incorporation efficiencies of viral RNA segments as described in notes *b* and *c*. The results shown are representative data from three independent experiments.

[b] VLPs and WSN helper virus were used to infect MDCK cells. With helper virus providing polymerase proteins and wild-type NP, GFP-positive MDCK cells represented VLPs that possessed at least one vRNA, i.e., HA-GFP vRNA (Fig. 3).

[c] Infectious VLPs were used to infect MDCK-NP cells. In this approach, GFP expression from HA-GFP vRNA requires the expression of the PB2, PB1, and PA proteins from the respective vRNA segments. GFP-positive MDCK cells therefore represented VLPs that contained at least four vRNAs (i.e., the HA-GFP, PB1, PB2, and PA vRNAs).

determined by counting the cells expressing GFP at 16 h postinfection. As shown in Table 2, the number of VLPs possessing HA-GFP vRNA produced from cells expressing R74A, R156A, R175A, R195A, R199A, or R361A was at least as high as that from cells expressing wild-type NP. These results suggest that the mutations had no or little effect on the incorporation efficiency of a single vRNA segment into VLPs. In contrast, cells expressing D72A, K113A, R174A, or K325A produced VLPs containing HA-GFP vRNA less efficiently than did the wild-type NP, indicating that these NP mutations may impair vRNA incorporation into VLPs, resulting in the observed failure of virus rescue.

Incorporation efficiency of multiple vRNA segments into VLPs containing mutant NPs. As described above, we found that R74A, R156A, R175A, R195A, R199A, and R361A support VLP incorporation of a single vRNA segment, leaving in question why these viruses replicate poorly. A possible explanation is that the NP mutant facilitates virion incorporation of single, but not multiple, vRNA segment. In such a scenario, the NP would assemble vRNA segments into sets of eight (in the form of RNPs) that constitute a functional genome. To examine this possibility, we generated an MDCK cell line stably expressing wild-type NP and used the cell line for VLP infection. Since a helper virus was not used for this experiment, PA, PB1, and PB2 vRNA segments had to be provided by incoming VLPs to support the replication/transcription of HA-GFP vRNA. The number of GFP-expressing cells should, therefore, correspond to the number of VLPs possessing at least four vRNAs (i.e., PA, PB1, PB2, and HA-GFP vRNAs). As shown in Table 2, we found that the number of VLPs possessing at least four vRNAs produced from cells expressing R74A, R156A, R175A, R195A, R199A, or R361A was significantly lower than that from cells expressing wild-type NP. These results suggest that these mutations affect the efficient incorporation of multiple vRNA segments into VLPs, even though they had no or little effect on the virion incorporation of a single vRNA. As expected, the mutations D72A, K113A, R174A, and K325A completely inhibited VLP incorporation of four vRNAs.

DISCUSSION

In this study, we conducted a comprehensive mutational analysis to examine the roles of highly conserved amino acids in the influenza A virus NP for the virus life cycle. We found 17 amino acid substitutions (i.e., R19A, Y40A, L49A, R98A, G132A, S141A, G169A, R214A, V242A, P277A, F291A, N319A, C333A, K357A, E369A, G490A, and E495E) that had no or little effect on virus growth in vitro at either 33°C or 37°C, whereas other mutations tested significantly impaired viral replication efficiency. Using an in vitro replication assay, we identified 15 amino acid changes (i.e., R150A, R208A, R213A, E254A, A260R, K273A, A337R, E339A, R355A, A387R, Q405A, F412A, R416A, F488A, and F489A) that are crucial for viral-genome replication and/or transcription (Table 1). Several NP mutants supported efficient replication in an in vitro replication assay but were highly attenuated in their growth properties. Some of these mutants facilitated efficient virion incorporation of a single vRNA but not that of multiple vRNAs. This is the first report that suggests a role of an influenza virus protein in the assembly and/or virion incorporation of vRNA segments.

The genome of influenza A virus consists of eight RNA segments. Two packaging models have been proposed for the generation of infectious virions containing these eight vRNA segments: "random-packaging" and "selective-packaging" models (9, 10, 37). Recently, it has been suggested that each vRNA segment of influenza A viruses contains specific incorporation signals for the recruitment and/or packaging of vRNPs into virions (6, 7, 11–13, 20, 21, 28, 36). These data support the "selective-packaging" mechanism of vRNA recruitment into virions. However, the involvement of other factors (i.e., viral proteins and/or host proteins) in the selective incorporation of the eight vRNPs into progeny virions is still poorly understood. In this study, we found 10 mutations (D72A, R74A, K113A, R156A, R174A, R175A, R195A, R199A, K325A, and R361A) that impaired the efficient incorporation of a set of at least four vRNAs (PA, PB1, PB2, and HA-GFP vRNP) into VLPs, although they did not affect the VLP incorporation of a single vRNA, i.e., the HA-GFP vRNA (Table 2). As shown in Fig. 4, eight of these NP mutations (i.e., D72A, K113A, R156A, R174A, R175A, R195A, R199A, and R361A) cluster around a possible RNA-binding groove that lies between the head and body domains at the exterior of the NP oligomer and is lined with highly conserved basic residues (41). Two of these residues (R74 and K325) are located in an internal domain of NP. The architecture of RNP complexes in influenza A virus particles is such that the RNPs are organized in a distinct pattern of seven segments of different lengths surrounding a central segment. Close contact has been shown between the peripheral RNPs, as well as the central and peripheral RNPs (26). NP may be involved in this close contact among the peripheral RNPs,

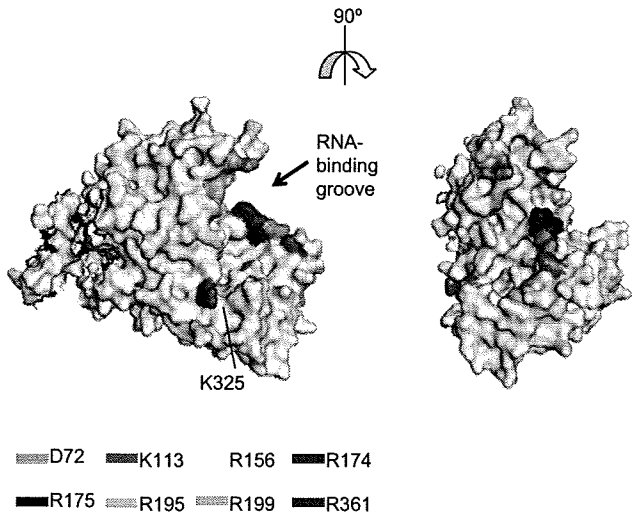

FIG. 4. Crystal structure of influenza A virus NP. The images were created with the program PYMOL (W. L. Delane; http://www.pymol.org), and the NP structure was obtained from the Protein Data Bank (41) (accession number 2IQH). The locations of the amino acid residues that affect the efficient incorporation of multiple vRNA segments into VLPs are shown in color.

through the interaction of RNPs and/or other essential host cellular components, leading to the efficient incorporation of the eight vRNA segments into virus particles.

Influenza A virus NP has at least two NLS sequences. An unconventional NLS is located between residues 3 and 13 and is responsible for NP binding to karyopherins α1 and α2 (35). The second NLS is a bipartite signal located in the middle of NP (residues 198 to 216) (37). The bipartite NLS can function as an NLS to a limited extent when it is fused to a cytoplasmic reporter protein (37). Its contribution to NP nuclear import, however, is not as significant as that of NLS1 (37). In this study, we attempted to generate five viruses that possessed amino acid substitutions in the bipartite NLS (R199A, R208A, R213A, R214A, and R216A). The R208A and R213A mutant viruses were not recoverable because these mutations significantly reduced viral transcription, consistent with a previous report that the bipartite NLS was essential for vRNA transcription (31). In contrast, the single amino acid substitution R214A or R216A had no effect on viral-genome replication/transcription, NP localization, or virus replication. These results suggest that a single mutation at position 214 or 216 of NP may not be sufficient to affect NP function, although multiple amino acid changes in the bipartite NLS (positions 213, 214, and 216) completely disrupt vRNA transcription, NP nuclear accumulation, and virus replication (31). We also found that a mutation at position 199 did not affect viral-genome replication/transcription and NP nuclear transport.

In this study, we found that mutations A337R, E339A, Q405A, S407A, F412A, V414A, R416A, F488A, F489A, D491A, and E495A significantly decreased the transcription of influenza vRNA (Table 1). The crystal structure of influenza NP shows that each NP contains a tail loop, formed by residues 402 to 428 (41). This tail loop is inserted into the body domain of a neighboring molecule in a counterclockwise direction when viewed along the threefold axis from the side of the head domain. Mutagenesis revealed that the tail loop is essential for NP oligomerization, which in turn is necessary for vRNA transcription (8, 42). Since the mutations we tested (A337R, E339A, Q405A, S407A, F412A, V414A, R416A, F488A, F489A, D491A, and E495A) reside in or near the NP-NP-interacting region (8, 41), they may disrupt the NP-NP interaction, leading to inhibition of viral-genome replication and transcription.

Using coimmunoprecipitation, Biswas et al. showed that coexpression of the components of the polymerase protein complex (PB1, PB2, or PA) with NP either together or pairwise revealed that NP interacts with PB1 and PB2 but not with PA (3). These experiments implicated three NP regions—amino acids 1 to 160, 256 to 340, and 340 to 498—in binding to the PB2 subunit of the viral polymerase (3, 33). In our study, mutant viruses R150A, E254A, A260R, K273A, A337A, E339A, R355A, A387R, Q405A, F412A, R416A, F488A, and F489A were not viable, and their abilities to support vRNA transcription were decreased significantly. Our results suggest that these NP mutations (i.e., R150A, E254A, A260R, K273A, A337A, E339A, R355A, A387R, Q405A, F412A, R416A, F488A, and F489A, which lie in or near the PB2 binding domain) block the interaction of NP with the polymerase subunits (PB1 and PB2), leading to defective viral growth.

In summary, we have identified amino acids that alter the functionality of NP in viral-genome replication/transcription. We have also identified amino acids in NP that facilitate efficient incorporation of multiple vRNA segments into progeny virions, suggesting a role of these amino acid residues in the assembly of influenza A virus segments in the form of RNPs. Further analyses of the significance of NP should provide information essential to our understanding of influenza virus replication.

ACKNOWLEDGMENTS

We thank Susan Watson for editing the manuscript and Krisna Wells and Martha McGregor for excellent technical assistance. We also thank Bill Sudgen for kindly providing plasmids.

This work was supported in part by U.S. National Institute of Allergy and Infectious Diseases Public Health Service research grants, by a grant-in-aid for Specially Promoted Research, and by a contract research fund for the Program of Funding Research Centers for Emerging and Reemerging Infectious Diseases from the Ministry of Education, Culture, Sports, Science and Technology; by ERATO (Japan Science and Technology Agency); and by grants-in-aid from the Ministry of Health, Labor, and Welfare of Japan.

REFERENCES

1. **Albo, C., A. Valencia, and A. Portela.** 1995. Identification of an RNA binding region within the N-terminal third of the influenza A virus nucleoprotein. J. Virol. **69**:3799–3806.
2. **Avalos, R. T., Z. Yu, and D. P. Nayak.** 1997. Association of influenza virus NP and M1 proteins with cellular cytoskeletal elements in influenza virus-infected cells. J. Virol. **71**:2947–2958.
3. **Biswas, S. K., P. L. Boutz, and D. P. Nayak.** 1998. Influenza virus nucleoprotein interacts with influenza virus polymerase proteins. J. Virol. **72**:5493–5501.
4. **Deng, T., O. G. Engelhardt, B. Thomas, A. V. Akoulitchev, G. G. Brownlee, and E. Fodor.** 2006. Role of Ran binding protein 5 in nuclear import and assembly of the influenza virus RNA polymerase complex. J. Virol. **80**: 11911–11919.
5. **Digard, P., D. Elton, K. Bishop, E. Medcalf, A. Weeds, and B. Pope.** 1999. Modulation of nuclear localization of the influenza virus nucleoprotein through interaction with actin filaments. J. Virol. **73**:2222–2231.
6. **Dos Santos Afonso, E., N. Escriou, I. Leclercq, S. van der Werf, and N. Naffakh.** 2005. The generation of recombinant influenza A viruses expressing a PB2 fusion protein requires the conservation of a packaging signal overlapping the coding and noncoding regions at the 5′ end of the PB2 segment. Virology **341**:34–46.

7. **Duhaut, S. D., and J. W. McCauley.** 1996. Defective RNAs inhibit the assembly of influenza virus genome segments in a segment-specific manner. Virology **216**:326–337.
8. **Elton, D., L. Medcalf, K. Bishop, D. Harrison, and P. Digard.** 1999. Identification of amino acid residues of influenza virus nucleoprotein essential for RNA binding. J. Virol. **73**:7357–7367.
9. **Elton, D., M. Simpson-Holley, K. Archer, L. Medcalf, R. Hallam, J. McCauley, and P. Digard.** 2001. Interaction of the influenza virus nucleoprotein with the cellular CRM1-mediated nuclear export pathway. J. Virol. **75**:408–419.
10. **Enami, M., G. Sharma, C. Benham, and P. Palese.** 1991. An influenza virus containing nine different RNA segments. Virology **185**:291–298.
11. **Fujii, K., Y. Fujii, T. Noda, Y. Muramoto, T. Watanabe, A. Takada, H. Goto, T. Horimoto, and Y. Kawaoka.** 2005. Importance of both the coding and the segment-specific noncoding regions of the influenza A virus NS segment for its efficient incorporation into virions. J. Virol. **79**:3766–3774.
12. **Fujii, Y., H. Goto, T. Watanabe, T. Yoshida, and Y. Kawaoka.** 2003. Selective incorporation of influenza virus RNA segments into virions. Proc. Natl. Acad. Sci. USA **100**:2002–2007.
13. **Gog, J. R., S. Afonso Edos, R. M. Dalton, I. Leclercq, L. Tiley, D. Elton, J. C. von Kirchbach, N. Naffakh, N. Escriou, and P. Digard.** 2007. Codon conservation in the influenza A virus genome defines RNA packaging signals. Nucleic Acids Res. **35**:1897–1907.
14. **Honda, A., K. Ueda, K. Nagata, and A. Ishihama.** 1988. RNA polymerase of influenza virus: role of NP in RNA chain elongation. J. Biochem. **104**:1021–1026.
15. **Huang, T. S., P. Palese, and M. Krystal.** 1990. Determination of influenza virus proteins required for genome replication. J. Virol. **64**:5669–5673.
16. **Katz, J. M., M. Wang, and R. G. Webster.** 1990. Direct sequencing of the HA gene of influenza (H3N2) virus in original clinical samples reveals sequence identity with mammalian cell-grown virus. J. Virol. **64**:1808–1811.
17. **Kennedy, G., and B. Sugden.** 2003. EBNA-1, a bifunctional transcriptional activator. Mol. Cell. Biol. **23**:6901–6908.
18. **Kobasa, D., M. E. Rodgers, K. Wells, and Y. Kawaoka.** 1997. Neuraminidase hemadsorption activity, conserved in avian influenza A viruses, does not influence viral replication in ducks. J. Virol. **71**:6706–6713.
19. **Kobayashi, M., T. Toyoda, D. M. Adyshev, Y. Azuma, and A. Ishihama.** 1994. Molecular dissection of influenza virus nucleoprotein: deletion mapping of the RNA binding domain. J. Virol. **68**:8433–8436.
20. **Liang, Y., Y. Hong, and T. G. Parslow.** 2005. *cis*-Acting packaging signals in the influenza virus PB1, PB2, and PA genomic RNA segments. J. Virol. **79**:10348–10355.
21. **Marsh, G. A., R. Hatami, and P. Palese.** 2007. Specific residues of the influenza A virus hemagglutinin viral RNA are important for efficient packaging into budding virions. J. Virol. **81**:9727–9736.
22. **Martin, K., and A. Helenius.** 1991. Nuclear transport of influenza virus ribonucleoproteins: the viral matrix protein (M1) promotes export and inhibits import. Cell **67**:117–130.
23. **Mena, I., E. Jambrina, C. Albo, B. Perales, J. Ortin, M. Arrese, D. Vallejo, and A. Portela.** 1999. Mutational analysis of influenza A virus nucleoprotein: identification of mutations that affect RNA replication. J. Virol. **73**:1186–1194.
24. **Neumann, G., T. Watanabe, H. Ito, S. Watanabe, H. Goto, P. Gao, M. Hughes, D. R. Perez, R. Donis, E. Hoffmann, G. Hobom, and Y. Kawaoka.** 1999. Generation of influenza A viruses entirely from cloned cDNAs. Proc. Natl. Acad. Sci. USA **96**:9345–9350.
25. **Niwa, H., K. Yamamura, and J. Miyazaki.** 1991. Efficient selection for high-expression transfectants with a novel eukaryotic vector. Gene **108**:193–199.
26. **Noda, T., H. Sagara, A. Yen, A. Takada, H. Kida, R. H. Cheng, and Y. Kawaoka.** 2006. Architecture of ribonucleoprotein complexes in influenza A virus particles. Nature **439**:490–492.
27. **Noton, S. L., E. Medcalf, D. Fisher, A. E. Mullin, D. Elton, and P. Digard.** 2007. Identification of the domains of the influenza A virus M1 matrix protein required for NP binding, oligomerization and incorporation into virions. J. Gen. Virol. **88**:2280–2290.
28. **Odagiri, T., and M. Tashiro.** 1997. Segment-specific noncoding sequences of the influenza virus genome RNA are involved in the specific competition between defective interfering RNA and its progenitor RNA segment at the virion assembly step. J. Virol. **71**:2138–2145.
29. **O'Neill, R. E., J. Talon, and P. Palese.** 1998. The influenza virus NEP (NS2 protein) mediates the nuclear export of viral ribonucleoproteins. EMBO J. **17**:288–296.
30. **Onishi, M., S. Kinoshita, Y. Morikawa, A. Shibuya, J. Phillips, L. L. Lanier, D. M. Gorman, G. P. Nolan, A. Miyajima, and T. Kitamura.** 1996. Applications of retrovirus-mediated expression cloning. Exp. Hematol. **24**:324–329.
31. **Ozawa, M., K. Fujii, Y. Muramoto, S. Yamada, S. Yamayoshi, A. Takada, H. Goto, T. Horimoto, and Y. Kawaoka.** 2007. Contributions of two nuclear localization signals of influenza A virus nucleoprotein to viral replication. J. Virol. **81**:30–41.
32. **Parvin, J. D., P. Palese, A. Honda, A. Ishihama, and M. Krystal.** 1989. Promoter analysis of influenza virus RNA polymerase. J. Virol. **63**:5142–5152.
33. **Portela, A., and P. Digard.** 2002. The influenza virus nucleoprotein: a multifunctional RNA-binding protein pivotal to virus replication. J. Gen. Virol. **83**:723–734.
34. **Stegmann, T., J. M. White, and A. Helenius.** 1990. Intermediates in influenza induced membrane fusion. EMBO J. **9**:4231–4241.
35. **Wang, P., P. Palese, and R. E. O'Neill.** 1997. The NPI-1/NPI-3 (karyopherin alpha) binding site on the influenza a virus nucleoprotein NP is a nonconventional nuclear localization signal. J. Virol. **71**:1850–1856.
36. **Watanabe, T., S. Watanabe, T. Noda, Y. Fujii, and Y. Kawaoka.** 2003. Exploitation of nucleic acid packaging signals to generate a novel influenza virus-based vector stably expressing two foreign genes. J. Virol. **77**:10575–10583.
37. **Weber, F., G. Kochs, S. Gruber, and O. Haller.** 1998. A classical bipartite nuclear localization signal on Thogoto and influenza A virus nucleoproteins. Virology **250**:9–18.
38. **Whittaker, G., M. Bui, and A. Helenius.** 1996. Nuclear trafficking of influenza virus ribonucleoproteins in heterokaryons. J. Virol. **70**:2743–2756.
39. **Wright, P. F., G. Neumann, and Y. Kawaoka.** 2007. Orthomyxoviruses, p. 1691–1740. *In* D. M. Knipe, P. M. Howley, D. E. Griffin, R. A. Lamb, M. A. Martin, B. Roizman, and S. E. Straus (ed.), Fields virology, 5th ed. Lippincott Williams & Wilkins, Philadelphia, PA.
40. **Yasuda, J., S. Nakada, A. Kato, T. Toyoda, and A. Ishihama.** 1993. Molecular assembly of influenza virus: association of the NS2 protein with virion matrix. Virology **196**:249–255.
41. **Ye, Q., R. M. Krug, and Y. J. Tao.** 2006. The mechanism by which influenza A virus nucleoprotein forms oligomers and binds RNA. Nature **444**:1078–1082.
42. **Ye, Z., T. Liu, D. P. Offringa, J. McInnis, and R. A. Levandowski.** 1999. Association of influenza virus matrix protein with ribonucleoproteins. J. Virol. **73**:7467–7473.

JOURNAL OF VIROLOGY, July 2009, p. 6429–6434
0022-538X/09/$08.00+0 doi:10.1128/JVI.00293-09

Vol. 83, No. 13

RuvB-Like Protein 2 Is a Suppressor of Influenza A Virus Polymerases▽

Satoshi Kakugawa,[1] Masayuki Shimojima,[1] Gabriele Neumann,[2] Hideo Goto,[1] and Yoshihiro Kawaoka[1,2,3,4]*

Division of Virology, Department of Microbiology and Immunology, Institute of Medical Science, University of Tokyo, 4-6-1 Shirokaneda, Minato-ku, Tokyo 108-8639, Japan[1]; Department of Pathobiological Sciences, School of Veterinary Medicine, University of Wisconsin, Madison, Wisconsin 53706[2]; Exploratory Research for Advanced Technology, Japan Science and Technology Agency, Saitama 332-0012, Japan[3]; and International Research Center for Infectious Diseases, Institute of Medical Science, University of Tokyo, Tokyo 108-8639, Japan[4]

Received 10 February 2009/Accepted 6 April 2009

In pro- and eukaryotic cells, RuvB-like protein 2 (RBL2) resolves Holliday junction recombination intermediates. Here, we identified RBL2 as a suppressor of influenza A virus replication. Human RBL2 appears to interfere with the oligomerization of the viral nucleoprotein, a critical step in the assembly of viral replication complexes.

Influenza A virus is an enveloped virus that belongs to the *Orthomyxoviridae* family and contains eight negative-sense RNA segments encoding 10 to 11 proteins (16). The RNA polymerase complex consists of three subunits, PB1, PB2, and PA. These polymerase subunits and nucleoprotein (NP), together with the viral RNA (vRNA), form the viral ribonucleoprotein complex (vRNP), which is the minimum component for vRNA replication and transcription.

Although some host factors have now been identified that interact with viral proteins (reviewed in reference 14), relatively little is known about the interplay between virus and host factors. We therefore developed a screening system to identify host proteins in a functional assay. Of the candidates that we identified that regulate virus RNA synthesis, RuvB-like protein 2 (RBL2) was identified as an inhibitor of vRNA synthesis.

RBL proteins (RBL1 and RBL2) are members of the AAA+ (ATPases associated with diverse cellular activities) family of helicases. They share moderate homology with bacterial RuvB, the ATP-dependent motor of the RuvAB complex that drives branch migration of the holiday junction (4). RBL1 and RBL2 are essential for viability in *Saccharomyces cerevisiae* and *Drosophila melanogaster* and may have similarly important roles in humans (1, 10).

In mammalian cells, the RBL proteins modulate cellular transformation, signaling, apoptosis, and the response to DNA damage by interacting with proteins such as β-catenin, c-Myc, and ATF2 (1, 2, 21). Moreover, they modulate rRNA processing and small nucleolar RNA maturation (12, 20) and function in complexes such as the chromatin remodeling complex INO80 (18) and the histone acetylase Tip60 complex (9).

Here, we provide evidence that RBL2 inhibits influenza virus replication. The protein interacts with the viral NP protein and interrupts its oligomerization, leading to inhibition of viral polymerase activity.

* Corresponding author. Mailing address: International Research Center for Infectious Diseases, Institute of Medical Science, University of Tokyo, Tokyo 108-8639, Japan. Phone: 81 3 5449 5310. Fax: 81 3 5449 5408. E-mail: kawaoka@ims.u-tokyo.ac.jp.

▽ Published ahead of print on 15 April 2009.

MATERIALS AND METHODS

Cell culture and viruses. Human embryonic kidney cells (293T cells and 293 cells) were cultured in Dulbecco's modified Eagle's medium (Sigma) supplemented with 10% heat-inactivated fetal calf serum and antibiotics. QT6 quail fibrosarcoma cells were maintained in Ham's F12K medium (MP Biomedicals) supplemented with 10% fetal calf serum and 10% tryptose phosphate broth (Sigma). Madin-Darby canine kidney (MDCK) cells were cultured in minimal essential medium containing 5% newborn calf serum and antibiotics. A/WSN/33 virus ([WSN] H1N1) was generated by reverse genetics (15) and propagated in MDCK cells. Viruses were titrated by plaque assay in MDCK cells.

Plasmids. The PB1, PB2, PA, and NP proteins of the A/Hong Kong/483/97 virus ([HK483] H5N1) were expressed using the pCAGGS vector (7) for the library screen. For all other experiments, these genes were derived from the WSN strain. The three polymerase cDNAs from the WSN strain fused to a c-Myc tag sequence at the 3′ termini and the NP cDNA from the WSN strain fused to a c-Myc tag sequence at the 5′ terminus were also inserted into pCAGGS. pPolI-GFP (where PolI is polymerase I and GFP is green fluorescent protein) drives the synthesis of negative-sense vRNAs comprising the 3′ noncoding region of the neuraminidase (HK483) vRNA, the complementary coding sequence of enhanced GFP (EGFP), and the 5′ noncoding region of the neuraminidase vRNA. Similarly, PolI-Luc drives the transcription of a virus-like RNA expressing luciferase.

Quail RBL2 (qRBL2) was cloned from QT6 cells by using the 5′ RACE System (Invitrogen) according to the manufacturer's instructions. Human RBL2 and RBL1 (hRBL2 and hRBL1, respectively) were cloned from human 293T cells. Briefly, RNA was extracted from these cells by use of an RNeasy Mini Kit (Qiagen). Reverse transcription-PCR (RT-PCR) was performed using an oligo(dT) primer, followed by PCR with gene-specific primers. hRBL2-DN (D299N) (2), which is designed to inactivate helicase activity, was constructed by using site-directed mutagenesis. These PCR products were cloned into the pCAGGS vector and then sequenced.

To assess the interaction between hRBL2 and the viral polymerase in living cells, we used a CoralHue Fluo-Chase kit (Amalgaam). Using the vectors in this kit, we constructed plasmids for the expression of the three polymerases, NP, and hRBL2 fused with the N- or C-terminal portion of Kusabira-Green, resulting in GN and GC fusion proteins (for example, pPB1-GN or pPB1-GC).

Library screening. Human embryonic kidney 293T cells were transfected with HK483 polymerase and NP protein expression plasmids (note that PB2 possesses glutamic acid at position 627), with a plasmid for the synthesis of a virus-like RNA encoding EGFP (PolI-EGFP) and with the quail QT6 cDNA library. Cells were incubated for 2 days at 33°C and collected, and GFP-expressing cells were sorted by a FACSCalibur instrument (BD). Plasmid DNA was then extracted from the cells and amplified in *Escherichia coli*. Cells that expressed high levels of GFP underwent selection three times, at which point their plasmid DNA was extracted and sequenced.

Luciferase assay. Luciferase assays were performed by use of a dual-luciferase reporter assay system (Promega) on a microplate luminometer (Veritas; Turner Biosystems, Sunnyvale, CA), according to the manufacturer's instructions. The

internal control for the dual-luciferase assay was pGL4.74(hRluc/TK) (Promega).

Analysis of virus propagation. To establish virus growth rates, three wells of 293 cells were transfected with the respective plasmid or small interfering RNA (siRNA) and 24 h (plasmid) or 48 h (siRNA) later infected with WSN at a multiplicity of infection (MOI) of 0.05. The cells were maintained at 37°C. At various time points, supernatants were assayed for virus titers by plaque assay in MDCK cells.

Knockdown of hRBL2 by use of siRNA. siRNA specific to RBL2 (catalog no. HSS116737) was purchased from Invitrogen. At 48 h posttransfection with the siRNA, cells were tested for RBL2 expression levels by Western blot analysis.

Quantification of vRNA products. To assess viral polymerase activity, cells transfected with protein expression plasmids or siRNAs were infected with WSN at an MOI of 2. At various time points, cells were washed three times with phosphate-buffered saline, after which the RNA was extracted and subjected to RT-PCR with NP gene-specific primers (sequences will be provided upon request) or oligo(dT) primers. The resultant cDNAs were quantified with LightCycler, version 2.0 (Roche), by NP gene-specific primers; beta-actin-specific primers served as an internal control.

Western blot analysis. To assess hRBL2 expression levels, cells transfected with the respective hRBL2 protein expression plasmid were suspended in Tris-glycine–sodium dodecyl sulfate (SDS) sample buffer (Invitrogen) and subjected to Western blot analysis with anti-hRBL2 (BD Transduction Laboratories) and anti-beta-actin (as an internal control; Sigma) antibodies, according to the manufacturer's instructions. Biotinylated anti-mouse immunoglobulin G (IgG) antibody (Vector) was used as a secondary antibody. Bands were detected using a Vectastain ABC kit (Vector) and ECL Plus Western Blotting Detection Reagents (GE Healthcare); the VersaDoc Imaging System (Bio-Rad) was used to quantify band intensities.

To analyze the expression of the viral M1 protein, cells transfected with protein expression plasmids or siRNA were infected with WSN at an MOI of 3 and incubated at 37°C. At the time points indicated in Fig. 2C or 3C, the cells were washed three times with phosphate-buffered saline and resuspended in Tris-glycine–SDS sample buffer. Western blot analysis was then performed with monoclonal antibodies specific to the M1 protein; beta-actin served as a control. Biotinylated anti-mouse IgG antibody (Vector) was used as a secondary antibody. Bands were detected as described above.

To assess the interaction of hRBL2 with viral polymerase complexes, 293T cells were transfected with plasmids for the expression of hRBL2 (pChRBL2), the viral polymerase proteins (pCAGGS-PB1, -PB2, and -PA), Myc-tagged NP protein, and, in a subset of experiments, a plasmid for the synthesis of virus-like RNA (PolI-GFP). Twenty-four hours later, Myc-tagged proteins were immunoprecipitated with anti-c-Myc agarose (Sigma). Nontagged NP served as a negative control. The beads were resuspended in Tris-glycine–SDS sample buffer, and Western blot analysis was performed with an antibody specific for hRBL2. Biotinylated anti-mouse IgG antibody (Vector) was used as a secondary antibody. Bands were detected as described above.

To assess the interaction of hRBL2 with individual components of the replication machinery, pChRBL2 was cotransfected with plasmids for the synthesis of Myc-tagged polymerase and NP proteins (pCPB1-Myc, pCPB2-Myc, pCPA-Myc, or pCMyc-NP). Immunoprecipitations were performed as described above.

BiFC assays. To examine the interaction of hRBL2 with viral proteins in living cells, we performed bimolecular fluorescence complementation (BiFC) assays using a CoralHue Fluo-Chase kit (Amalgaam). Briefly, the respective proteins were fused to N- or C-terminal portions of Kusabira-Green, resulting in GN or GC fusion proteins. Pairs of GN and GC fusion proteins were transfected into 293T cells and subjected 12 or 24 h later to luciferase assays or fluorescence-activated cell sorting (FACS) analysis, respectively.

RESULTS AND DISCUSSION

To identify host proteins that regulate viral replication, we developed a screening system in which human embryonic kidney 293T cells are transfected with a plasmid for the synthesis of a virus-like RNA encoding EGFP (PolI-EGFP) and with plasmids for the expression of the influenza A virus polymerase and NP proteins (Fig. 1). The PB2 protein possesses glutamic acid at position 627, which attenuates replication in mammalian systems at 33°C but allows efficient replication in avian systems (19). To identify avian host factors that rescue efficient

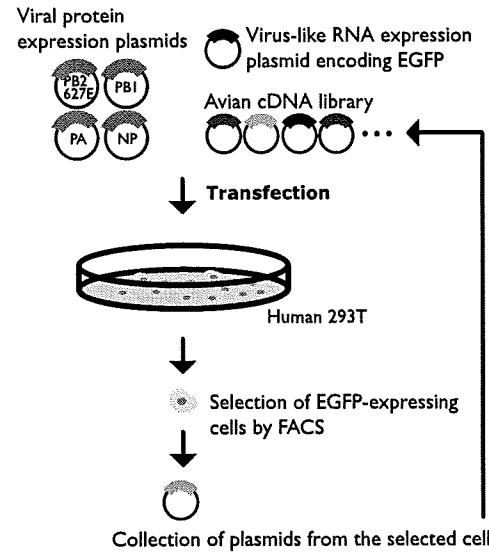

FIG. 1. Identification of cellular proteins that enhance influenza virus replication. Cells were transfected with plasmids encoding the HK483 (H5N1) PB2, PB1, PA, and NP proteins (the PB2 protein possesses glutamic acid at position 627; PB2-627E). Cells were cotransfected with PolI-EGFP for the synthesis of a virus-like RNA and with an avian (quail cell) cDNA expression library. Cells expressing avian proteins that support efficient replication by PB2-627E in mammalian cells at 33°C produce increased amounts of EGFP. GFP-expressing cells were selected by a FACS cell sorter. After three rounds of selection, plasmid DNA was extracted from the cells and sequenced.

replication, we cotransfected cells with a cDNA expression library derived from quail QT6 cells. Cells were incubated for 2 days at 33°C, and then GFP-expressing cells were sorted by FACSCalibur (BD). After three rounds of selection, we extracted plasmid DNAs and sequenced them. Among the quail proteins that upregulated viral replication was a truncated qRBL2 protein that lacked 217 N-terminal amino acids (ΔN-qRBL2).

A role for RBL proteins in the regulation of viral infections has not been described to date. However, using a genome-wide RNA interference screen in *Drosophila* to identify host genes important for influenza virus replication, we found that knockdown of the *Drosophila* homolog of hRBL2 enhanced reporter gene expression of the influenza virus replicon (6). In addition, Mayer et al. identified hRBL2 as a cellular interaction partner of influenza vRNPs (13). However, neither Hao et al. nor Mayer et al. assessed the biological significance of the RBL2 interaction with influenza vRNPs.

To confirm that ΔN-qRBL2 affects influenza virus RNA replication, we expressed it in human embryonic kidney (293) cells that also expressed the polymerase and NP proteins and a virus-like RNA encoding luciferase. Viral polymerase activity was indeed upregulated upon expression of ΔN-qRBL2 (Fig. 2A). We then overexpressed the full-length hRBL2 and qRBL2 in 293 cells that were subsequently infected with influenza virus strain WSN (H1N1) at an MOI of 1. Assessment of vRNA, cRNA, and mRNA levels by real-time RT-PCR at 3 h postinfection revealed downregulation of polymerase activity upon overexpression of hRBL2 or qRBL2 (Fig. 2B). As a consequence, viral protein synthesis (Fig. 2C) and replication

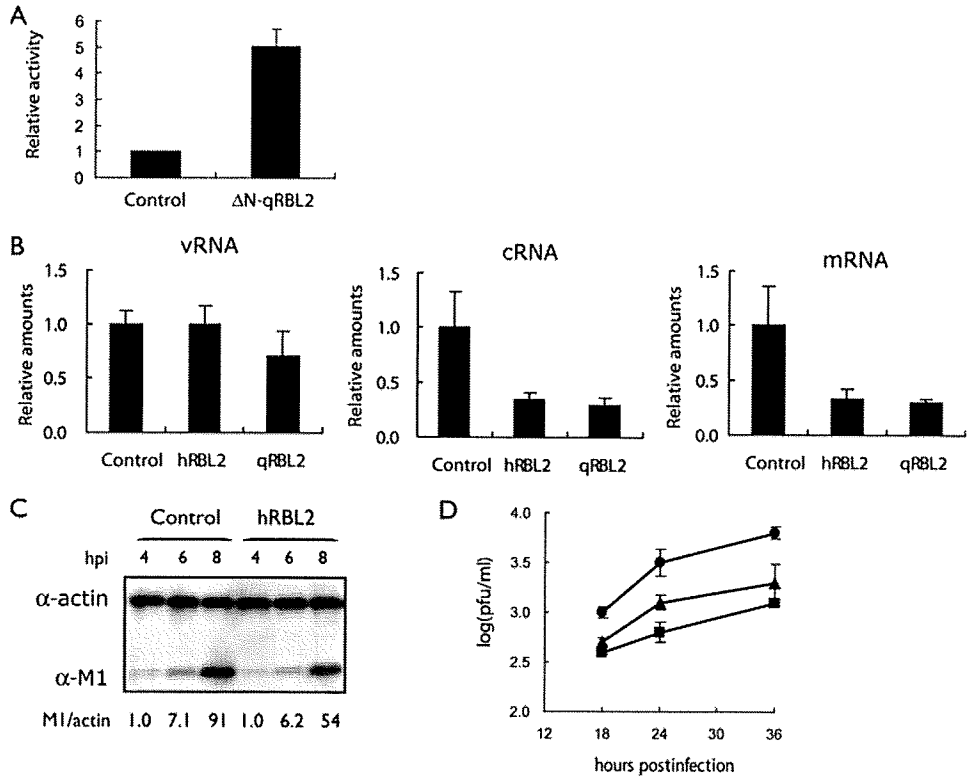

FIG. 2. Effect of RBL2 expression on influenza virus replication and growth. (A) ΔN-qRBL2 increases influenza virus replication in a minireplicon assay. 293T cells were transfected with plasmids expressing HK483 PB1, PB2-627K, PA, and NP proteins, pPolI-Luc, and ΔN-qRBL2. Twenty-four hours after incubation at 33°C, luciferase expression was detected. (B) Viral polymerase activity in cells expressing hRBL2 or qRBL2. 293 cells were transfected with plasmids expressing qRBL2 or hRBL2 or a control vector. Twenty-four hours later, cells were infected with strain WSN (MOI of 1). Three hours later, RNA was extracted and quantified by real-time RT-PCR with primer sets specific for NP vRNA, cRNA, or mRNA. These values were normalized to beta-actin. The error bars represent standard deviations ($n = 3$). (C) Viral M1 protein production in cells overexpressing hRBL2. 293 cells expressing hRBL2 or a control vector were infected with strain WSN (MOI of 3). At the indicated hours postinfection (hpi), cell lysates were subjected to Western blot analysis with antibodies against M1 and beta-actin. The values show the ratio of M1 to actin normalized to control cells 4 h after infection. (D) Influenza virus titers in 293 cells overexpressing hRBL2 or qRBL2. 293 cells overexpressing hRBL2 (square), qRBL2 (triangle), or a control vector (circle) were infected with strain WSN (MOI of 0.05). The cells were incubated at 37°C for the indicated time periods. Virus titers in the supernatant were determined by plaque assays in MDCK cells. The error bars represent standard deviations ($n = 3$). α, anti.

(Fig. 2D) were restricted. These findings indicate that ΔN-qRBL2 (identified in our screen) likely enhances influenza virus replication by acting as a dominant negative protein that competes with the endogenous RBL2 and that RBL2 is a general rather than host-species-specific host factor that suppresses influenza virus replication.

To further demonstrate that RBL2 interferes with influenza virus replication, we knocked it down in 293 cells by use of a specific siRNA (Fig. 3A, left and middle lanes). In these cells, the amounts of viral transcripts were increased relative to control cells (Fig. 3B, compare white and black bars), an effect that was partially reversed upon transfection of RBL2 siRNA-treated cells with a plasmid expressing hRBL2 (pChRBL2) (Fig. 3A, right lane, and B). Further, viral protein production and replication increased in RBL2 siRNA-treated cells (Fig. 3C and D), demonstrating that hRBL2 has an antiviral effect on influenza virus replication.

RBL2 possesses ATPase activity, which is critical for its biological function (2, 4). We therefore assessed a dominant negative form of RBL2 that lacks ATPase activity (hRBL2-DN) (2) for its effects on influenza virus growth. We found that hRBL2-DN interfered with polymerase activity and virus growth at almost the same level as the wild-type protein (data not shown). Hence, the ATPase activity of hRBL2 is not critical for its antiviral effect.

To investigate the interaction of hRBL2 with influenza vRNPs, we expressed hRBL2, the three polymerase subunits, and c-Myc-tagged NP protein in the absence or presence of a virus-like RNA. hRBL2 interacted with the viral replication complex regardless of the presence of vRNA (Fig. 4A). To assess which viral protein interacts with hRBL2, c-Myc-tagged polymerase and NP proteins were separately expressed with hRBL2 and immunoprecipitated with beads coated with an anti-c-Myc antibody. Interestingly, Western blot analysis showed that hRBL2 interacts with three different vRNP components—NP, PB2, and PB1 (Fig. 4B).

To further study the interaction of hRBL2 with vRNP components, we used a BiFC assay (8, 11) in which the proteins of interest were fused to N-terminal and C-terminal portions of Kusabira-Green (resulting in GN and GC fusion proteins, respectively); interaction of the proteins of interest thus resulted in Kusabira-Green fluorescence (Fig. 5A, upper panel). Strong

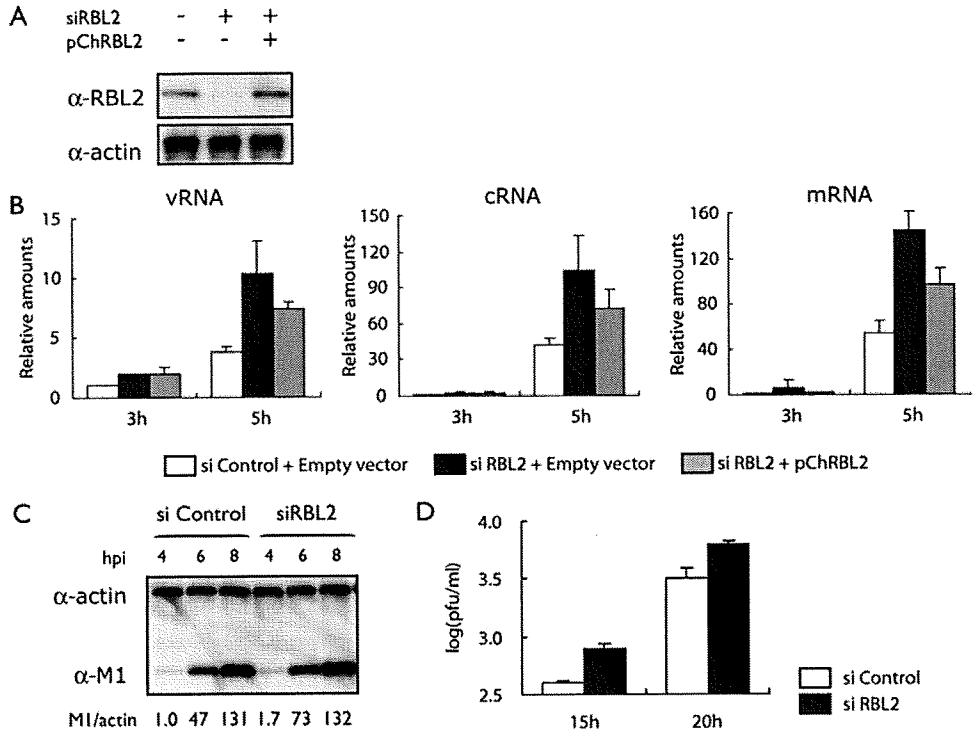

FIG. 3. Effect of hRBL2 knockdown on influenza virus replication. (A) Knockdown of hRBL2 in 293 cells. 293 cells were transfected with an siRNA specific to hRBL2 (siRBL2) or with a nonspecific control siRNA. Cells were also transfected with a plasmid expressing hRBL2 (pChRBL2) or a control vector. Two days later, hRBL2 expression levels were assessed by Western blot analysis. Beta-actin expression levels served as an internal control. (B) Viral polymerase activity in cells treated with an siRNA to hRBL2. 293 cells were transfected with hRBL2-specific or control siRNAs (si Control) and incubated at 37°C for 48 h. The transfected cells were then infected with strain WSN (MOI of 1). The amounts of vRNA, cRNA, and mRNA were determined at 5 h postinfection as described in the legend of Fig. 2b. (C) Viral M1 protein production in hRBL2 knockdown cells and control cells. Cells were transfected with siRNAs as described above and infected with WSN virus at an MOI of 3. M1 protein levels were assessed as described in the legend of Fig. 2c. (D) Influenza virus titers in hRBL2 knockdown cells and control cells. Cells were treated with siRNAs as described above, infected with WSN virus at an MOI of 0.05, and incubated at 37°C for the indicated time periods. Virus titers were determined in MDCK cells. The error bars represent standard deviations (n = 3). α, anti.

fluorescence was detected for the hRBL2 interaction with NP (Fig. 5A), whereas the level of fluorescence suggested no interaction or only moderate interaction of hRBL2 and the polymerase proteins in this assay.

NP was found to interact with hRBL2 in both the immunoprecipitation and BiFC assays. To assess if hRBL2 interferes with NP oligomerization, which is important for its biological activities (3, 22), we tested the NP-NP interaction in cells

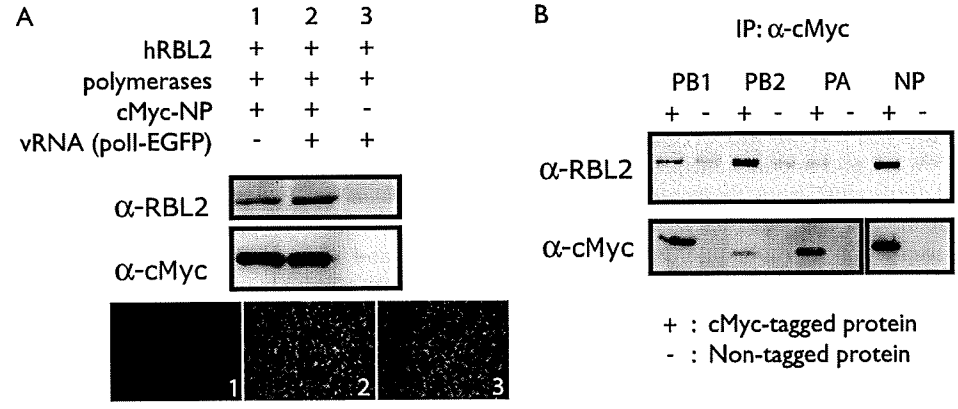

FIG. 4. Interaction of hRBL2 with viral proteins. (A) hRBL2 interacts with viral RNP complexes. The three viral polymerase proteins and c-Myc-tagged NP were expressed in 293T cells in the absence or presence of virus-like RNA (lanes 1 and 2). Nontagged NP was expressed as a negative control (lane 3). One day later, cell lysates were immunoprecipitated with anti-c-Myc beads. Western blot analysis was carried out with anti-hRBL2 and anti-c-Myc antibodies. EGFP expression in transfected cells indicates the functionality of c-Myc-tagged NP protein. (B) hRBL2 interacts with NP, PB2, and PB1. The three polymerase and NP proteins were individually tested for their interaction with hRBL2 as described above. α, anti; IP, immunoprecipitation.

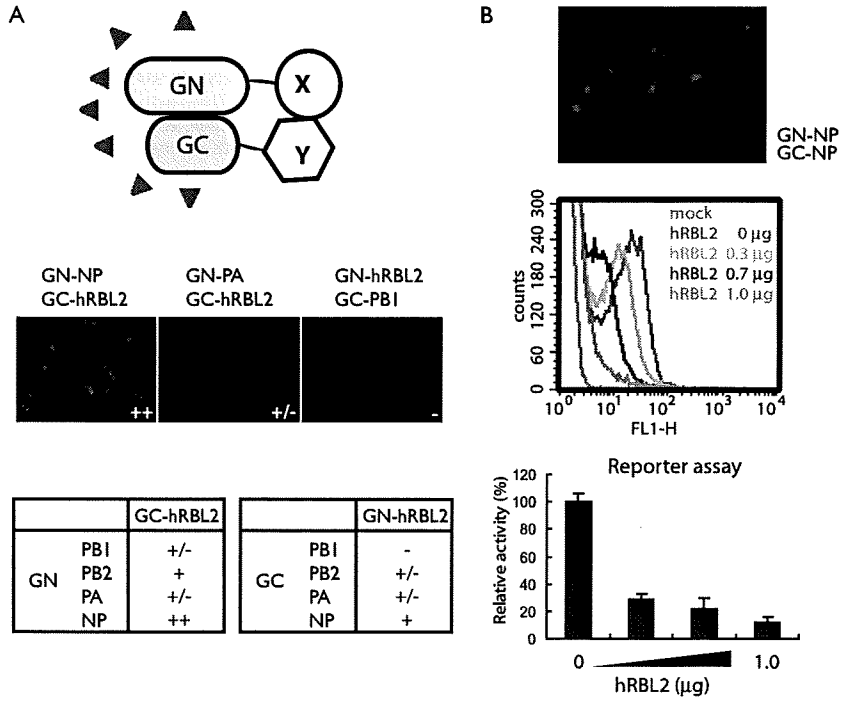

FIG. 5. hRBL2 interferes with NP oligomerization. (A) BiFC assay to assess interactions between hRBL2 and vRNP components. The proteins of interest were fused to the N- or C-terminal portions of Kusabira-Green (GN or GC). Interaction between the proteins of interest thus results in fluorescence. hRBL2 interacts with NP but not with the polymerase subunits. (B) hRBL2 inhibits NP oligomerization in a dose-dependent manner. Cells were transfected with plasmids for the expression of PB2, PB1, PA, pPolI-GFP, and GN-NP and GC-NP. NP-NP interaction was detected by microscopy and FACS analysis (middle panel, red curve). This interaction decreased with increasing amounts of hRBL2 (middle panel). Reporter gene expression in transfected cells indicates the functionality of the GN-NP and GC-NP fusion proteins and the biological significance of hRBL2 interference with NP oligomerization.

overexpressing hRBL2. As expected, we detected NP-NP interaction in the BiFC assay (Fig. 5B, upper panel); however, hRBL2 overexpression decreased the levels of fluorescence (indicative of NP-NP interaction) in a dose-dependent manner (Fig. 5B, middle panel). Similarly, reporter gene expression from a virus-like RNA was also reduced by hRBL2 expression in a dose-dependent manner (Fig. 5B, lower panel), demonstrating the functionality of NP fusion products and the biological significance of the hRBL2 interference with NP oligomerization. Collectively, these data suggest that hRBL2 disrupts the proper assembly of NP oligomers and, thereby, interrupts its biological activities. In addition to identifying this new host antiviral mechanism, our study also suggests RBL2 as a promising target for antiviral drug development.

Mammalian RBL proteins are implicated in a wide range of cellular activities, including DNA replication and repair, cell cycle progression, and chromatin remodeling (4). Structural analysis revealed that RBL2 and RBL1 can assemble into a double hexameric ring complex in vitro and that the dodecamer is likely one of the functional forms of the proteins (5, 17). Currently, it is not clear whether one of the hexamers contains exclusively RBL2 and the other RBL1 or whether both contain equimolar amounts of RBL2 and RBL1 (4). However, each protein is thought to have specific roles, and some data suggest subunit-specific functions that may not require RBL1/RBL2 complex formation (4). This is in line with findings by Mayer et al., who identified hRBL2, but not hRBL1, as a cellular interaction partner of vRNPs (13). Moreover, we did not detect a role for hRBL1 in influenza virus infection (data not shown). Hence, the inhibitory effect of hRBL2 on influenza virus seems to be a specific function of RBL2 rather than of the RBL1/RBL2 heterooligomer.

ACKNOWLEDGMENTS

We thank Susan Watson for editing the manuscript. We also thank H. Mimuro and N. Ishijima for technical support.

This research was supported by a Grant-in-Aid for Specially Promoted Research from the Ministry of Education, Culture, Sports, Science, and Technology of Japan; by a Grant-in-Aid for JSPS Fellows from the Japanese Society for the Promotion of Science (JSPS); by ERATO (Japan Science and Technology Agency); and by the National Institute of Allergy and Infectious Diseases Public Health Service research grants. S.K. was supported by JSPS Research Fellowships for Young Scientists.

REFERENCES

1. **Bauer, A., S. Chauvet, O. Huber, F. Usseglio, U. Rothbächer, D. Aragnol, R. Kemler, and J. Pradel.** 2000. Pontin52 and reptin52 function as antagonistic regulators of beta-catenin signalling activity. EMBO J. **19**:6121–6130.
2. **Cho, S. G., A. Bhoumik, L. Broday, V. Ivanov, B. Rosenstein, and Z. Ronai.** 2001. TIP49b, a regulator of activating transcription factor 2 response to stress and DNA damage. Mol. Cell. Biol. **21**:8398–8413.
3. **Elton, D., E. Medcalf, K. Bishop, and P. Digard.** 1999. Oligomerization of the influenza virus nucleoprotein: identification of positive and negative sequence elements. Virology **260**:190–200.
4. **Gallant, P.** 2007. Control of transcription by Pontin and Reptin. Trends Cell Biol. **17**:187–192.
5. **Gribun, A., K. L. Cheung, J. Huen, J. Ortega, and W. A. Houry.** 2008. Yeast Rvb1 and Rvb2 are ATP-dependent DNA helicases that form a heterohexameric complex. J. Mol. Biol. **376**:1320–1333.
6. **Hao, L., A. Sakurai, T. Watanabe, E. Sorensen, C. A. Nidom, M. A. Newton,**

P. Ahlquist, and Y. Kawaoka. 2008. *Drosophila* RNAi screen identifies host genes important for influenza virus replication. Nature **454**:890–893.
7. **Hatta, M., P. Gao, P. Halfmann, and Y. Kawaoka.** 2001. Molecular basis for high virulence of Hong Kong H5N1 influenza A viruses. Science **293**:1840–1842.
8. **Hu, C. D., and T. K. Kerppola.** 2003. Simultaneous visualization of multiple protein interactions in living cells using multicolor fluorescence complementation analysis. Nat. Biotechnol. **21**:539–545.
9. **Ikura, T., V. V. Ogryzko, M. Grigoriev, R. Groisman, J. Wang, M. Horikoshi, R. Scully, J. Qin, and Y. Nakatani.** 2000. Involvement of the TIP60 histone acetylase complex in DNA repair and apoptosis. Cell **102**:463–473.
10. **Kanemaki, M., Y. Kurokawa, T. Matsu-ura, Y. Makino, A. Masani, K. Okazaki, T. Morishita, and T. A. Tamura.** 1999. TIP49b, a new RuvB-like DNA helicase, is included in a complex together with another RuvB-like DNA helicase, TIP49a. J. Biol. Chem. **274**:22437–22444.
11. **Kerppola, T. K.** 2006. Complementary methods for studies of protein interactions in living cells. Nat. Methods **3**:969–971.
12. **King, T. H., W. A. Decatur, E. Bertrand, E. S. Maxwell, and M. J. Fournier.** 2001. A well-connected and conserved nucleoplasmic helicase is required for production of box C/D and H/ACA snoRNAs and localization of snoRNP proteins. Mol. Cell. Biol. **21**:7731–7746.
13. **Mayer, D., K. Molawi, L. Martínez-Sobrido, A. Ghanem, S. Thomas, S. Baginsky, J. Grossmann, A. García-Sastre, and M. Schwemmle.** 2007. Identification of cellular interaction partners of the influenza virus ribonucleoprotein complex and polymerase complex using proteomic-based approaches. J. Proteome Res. **6**:672–682.
14. **Nagata, K., A. Kawaguchi, and T. Naito.** 2008. Host factors for replication and transcription of the influenza virus genome. Rev. Med. Virol. **18**:247–260.
15. **Neumann, G., T. Watanabe, H. Ito, S. Watanabe, H. Goto, P. Gao, M. Hughes, D. R. Perez, R. Donis, E. Hoffmann, G. Hobom, and Y. Kawaoka.** 1999. Generation of influenza A viruses entirely from cloned cDNAs. Proc. Natl. Acad. Sci. USA **96**:9345–9350.
16. **Palese, P.** 2007. *Orthomyxoviridae*, p. 1647–1689. *In* D. M. Knipe, P. M. Howley, D. E. Griffin, R. A. Lamb, M. A. Martin, B. Roizman, and S. E. Straus (ed.), Fields virology, 5th ed. Lippincott Williams & Wilkins, Philadelphia, PA.
17. **Puri, T., P. Wendler, B. Sigala, H. Saibil, and I. R. Tsaneva.** 2007. Dodecameric structure and ATPase activity of the human TIP48/TIP49 complex. J. Mol. Biol. **366**:179–192.
18. **Shen, X., G. Mizuguchi, A. Hamiche, and C. Wu.** 2000. A chromatin remodelling complex involved in transcription and DNA processing. Nature **406**: 541–544.
19. **Shinya, K., S. Hamm, M. Hatta, H. Ito, T. Ito, and Y. Kawaoka.** 2004. PB2 amino acid at position 627 affects replicative efficiency, but not cell tropism, of Hong Kong H5N1 influenza A viruses in mice. Virology **320**:258–266.
20. **Watkins, N. J., I. Lemm, D. Ingelfinger, C. Schneider, M. Hossbach, H. Urlaub, and R. Lührmann.** 2004. Assembly and maturation of the U3 snoRNP in the nucleoplasm in a large dynamic multiprotein complex. Mol. Cell **16**:789–798.
21. **Wood, M. A., S. B. McMahon, and M. D. Cole.** 2000. An ATPase/helicase complex is an essential cofactor for oncogenic transformation by c-Myc. Mol. Cell **5**:321–330.
22. **Ye, Q., R. M. Krug, and Y. J. Tao.** 2006. The mechanism by which influenza A virus nucleoprotein forms oligomers and binds RNA. Nature **444**:1078–1082.